Mixed micelles of lipoic acid-chitosan-poly(ethylene glycol) and distearoylphosphatidylethanolamine-poly(ethylene glycol) for tumor delivery

Zeeneh Elsaid, Kevin M.G. Taylor, Sanyogitta Puri, Cath A. Eberlein, Khuloud Al-jamal, Jie Bai, Rebecca Klippstein, Julie Tzu-Wen Wang, Ben Forbes, Jasminder Chana, Satyanarayana Somavarapu

PII: S0928-0987(17)30063-5
DOI: doi: 10.1016/j.ejps.2017.02.001
Reference: PHASCI 3899

To appear in: *European Journal of Pharmaceutical Sciences*

Received date: 31 October 2016
Revised date: 27 January 2017
Accepted date: 1 February 2017

Please cite this article as: Zeeneh Elsaid, Kevin M.G. Taylor, Sanyogitta Puri, Cath A. Eberlein, Khuloud Al-jamal, Jie Bai, Rebecca Klippstein, Julie Tzu-Wen Wang, Ben Forbes, Jasminder Chana, Satyanarayana Somavarapu , Mixed micelles of lipoic acid-chitosan-poly(ethylene glycol) and distearoylphosphatidylethanolamine-poly(ethylene glycol) for tumor delivery. The address for the corresponding author was captured as affiliation for all authors. Please check if appropriate. Phasci(2017), doi: 10.1016/j.ejps.2017.02.001

Mixed micelles of lipoic acid-chitosan-poly(ethylene glycol) and distearoylphosphatidylethanolamine-poly(ethylene glycol) for tumor delivery

Zeeneh Elsaid[a**], Kevin M. G. Taylor[a], Sanyogitta Puri[b], Cath A. Eberlein[b], Khuloud Al-jamal[c], Jie Bai[c], Rebecca Klippstein[c], Julie Tzu-Wen Wang[c], Ben Forbes[c], Jasminder Chana[c], Satyanarayana Somavarapu[a*].

[a] UCL School of Pharmacy, 29-39 Brunswick Square, London, WC1N 1AX'

[b] AstraZeneca, Macclesfield, Cheshire East, SK10 2NA

[c] Kings College London, Franklin-Wilkins Building, Stamford Street, London, SE1 8WA

*Corresponding author (1): E-mail: s.somavarapu@ucl.ac.uk

**Corresponding author (2): E-mail: elsaid_a@hotmail.com

Conflict of interest, financial disclosures: This project was funded by a grant from AstraZeneca. Sanyogitta Puri and Cath A. Eberlein are employees of AstraZeneca, UK.

Abstract

Many chemotherapeutics suffer from poor aqueous solubility and tissue selectivity. Distearoylphosphatidylethanolamine-poly(ethylene glycol) (DSPE-PEG) micelles are a promising formulation strategy for the delivery of hydrophobic anticancer drugs. However, storage and *in vivo* instability restrict their use. The aim of this study was to prepare mixed micelles, containing a novel polymer, lipoic acid-chitosan-poly(ethylene glycol) (LACPEG), and DSPE-PEG, to overcome these limitations and potentially increase cancer cell internalisation. Drug-loaded micelles were prepared with a model tyrosine kinase inhibitor and characterized for size, surface charge, stability, morphology, drug entrapment efficiency, cell viability (A549 and PC-9 cell lines), *in vivo* biodistribution, ex vivo tumor accumulation and cellular internalisation. Micelles of size 30–130 nm with entrapment efficiencies of 46 – 81% were prepared. LACPEG/DSPE-PEG mixed micelles showed greater interaction with the drug (condensing to half their size following entrapment), greater stability, and a safer profile *in vitro* compared to DSPE-PEG micelles. LACPEG/ DSPE-PEG and DSPE-PEG micelles had similar entrapment efficiencies and *in vivo* tumor accumulation levels, but LACPEG/ DSPE-PEG micelles showed higher tumor cell internalisation. Collectively, these findings suggest that LACPEG/DSPE-PEG mixed micelles provide a promising platform for tumor delivery of hydrophobic drugs.

Keywords = Mixed micelles, cancer, hydrophobic drug, biodistribution, uptake, chitosan, DSPE-PEG

1. Introduction

Chemotherapeutic agents act via various mechanisms to inhibit tumor growth, angiogenesis and metastasis, as well as to increase cancer cell apoptosis. Poor aqueous solubility and bioavailability are key limitations for several of these agents that are administered via the oral route. In the clinic, in order to achieve therapeutic concentrations at the target site, dose escalation of the drug is sometimes employed (Farhat and Houhou, 2013; Xue et al., 2015) which is, in turn, associated with increased toxicity. Furthermore, poor aqueous solubility also prevents their administration intravenously, a route which may be considered for patients incapable of taking the drug orally. Thus, it would be extremely beneficial to develop alternative delivery systems for these agents.

Polymeric micelles (<100 nm), comprising amphiphilic polymers, are emerging as promising drug delivery vehicles for poorly water-soluble drugs (Kim et al., 2010). Their structure presents a number

of advantages; with their inner core aiding hydrophobic drug incorporation and the outer hydrophilic shell reducing particle aggregation and opsonisation (Torchilin, 2001), thereby hindering uptake by the reticuloendothelial system (Haag, 2004; Torchilin, 2007). The latter prolongs the circulation half-life, an effect which when considered with their small size, promotes passive accumulation at the tumor site as a result of the enhanced permeation and retention (EPR) effect (Maeda et al., 2013). These advantages for site-specific drug delivery could potentially improve the delivery of traditional and emerging chemotherapeutic drugs, which might otherwise have been abandoned due to insolubility and toxicity.

An increasing number of micelle formulations are under investigation in preclinical and clinical studies for the delivery of hydrophobic anticancer drugs. One such example is NK012, which has entered phase II clinical trials. This is a block copolymer of poly (ethylene glycol) (PEG) and polyglutamate conjugated to the drug, 7-ethyl-10-hydroxycampothecin (SN-38). This micellar system demonstrated promising results with an up to 5.8-fold higher IC50 values and lower clearance relative to free SN-38 (Burris et al., 2016; Koizumi et al., 2006). Another example is Genexol-PM, which has entered phase II clinical trials for NSCLC, and comprises polymeric micelles composed of PEG and poly(D,L-lactic acid), and was shown to enhance the maximum tolerated dose and antitumor efficacy of paclitaxel (Kim et al., 2001). This micellar formulation has also reached the market in a number of places, including Korea and Europe (Pillai, 2014). Also, Afatinib within micelles, prepared from a polymer blend of MPEG-PCL/Mal-PEG-PCL, demonstrated higher cytotoxic activity and growth suppression in tumours obtained from colorectal cancer patients than compared to drug solution alone (Guan et al., 2014).

All of these micelles contain PEG, which provides steric hindrance, reducing aggregation and physically stabilising the preparations. It also reduces clearance by the reticuloendothelial system, improving the drug/micelle circulation half-life and allowing it to reach the tumor site post intravenous injection (Alexis et al., 2008; Maeda et al., 2000; Maruyama, 2011). Micelles composed of PEG and phospholipids, such as Distearoylphosphatidylethanolamine-poly(ethylene glycol) (DSPE-PEG), have generated considerable interest due to their small size which promotes passive accumulation at the target site secondary to the EPR effect (Diao et al., 2011; Maeda, 2001; Matsumura and Maeda,

1986), prolonged circulation half-life (Maruyama et al., 1992), enhanced cellular uptake (Wang et al., 2012), reduced toxicity (Deol and Khuller, 1997) and high loading (of up to 95%) of hydrophobic anticancer drugs (Sezgin et al., 2006; Wang et al., 2012). However, storage and *in vivo* instability limit their use and hinder their translation into the clinic. Storage of DSPE-PEG micellar solutions for longer than 1 week, at 25°C, results in carrier instability and precipitate formation (Johnsson et al., 2001). Additionally, following injection *in vivo*, DSPE-PEG micelle destabilization may occur due to significant dilution (critical micelle concentration is 0.5-1 μM (Ashok et al., 2004)), an outcome which is exacerbated by serum proteins, such as bovine serum albumin (BSA), which interact with the hydrophobic components of the micelles (Castelletto et al., 2007; Kastantin et al., 2010), resulting in the premature release of the encapsulated agents prior to the micelles reaching their target site. Previous studies have shown that the use of two or more amphiphilic polymers, to prepare mixed micelles, can overcome these limitations; micelles possess greater *in vivo* stability, as the hydrophobic components of the carrier are screened by the di-block mPEG component of the micelles, reducing its interaction with the BSA and efficiently preventing BSA adsorption onto the mixed micelles (Li et al., 2011). Mixed micelles have also shown greater storage stability, attributed to the increased interactions between the hydrophobic chains in the micellar core which stabilize the structure, or to specific polymer characteristics, such as PEG content (Gao et al., 2008; Li et al., 2011; Zheng et al., 2016). Mixed micelles also provide the added advantages of improved drug loading and cellular uptake, as demonstrated for a range of hydrophobic drugs (Attia et al., 2013; Butt et al., 2012; Cao et al., 2016; Kahook et al., 2010; Yang, 2010). Moreover, the FDA has Doxil®, an intravenously administered liposome formulation of the cytotoxic drug doxorubicin, with three lipid components, including DSPE-PEG.

A second novel polymer, lipoic acid-chitosan-poly(ethylene glycol) LACPEG, with desirable properties to overcome the stability limitations of conventional micelles, can be used with DSPE-PEG to form mixed micelles with potential to improve hydrophobic drug delivery. The design of LACPEG was informed by a number of factors. Lipoic acid has antioxidant and anti-inflammatory activities (Weerakody et al., 2008), which could help to reduce oxidative stress and inflammation, two crucial pathways involved in carcinogenesis (Reuter et al., 2010). It has also been shown to inhibit cell proliferation (by inhibiting the Akt pathway and up-regulating a cyclin-dependent kinase inhibitor) and

growth (by inhibiting tyrosine phosphorylation, and hence activation of growth factor receptors), as well inducing the selective apoptosis of a number of cancer cell lines, such as colon and lung cancer, (by increasing caspase activity, increasing the uptake of oxidizable substrates into the mitochondria and changing the ratio of the apoptotic-related protein Bax/Bcl-2) (Choi et al., 2009; Dozio et al., 2010; Michikoshi et al., 2013; Na et al., 2009; Wenzel et al., 2005). These properties could help to augment those of the drug and result in a greater inhibition of tumor cell growth. Chitosan was selected for its mucoadhesive, antioxidant, antiangiogenic and wound-healing properties (Sogias et al., 2008; Xu et al., 2009; Yen et al., 2008), as well as its polycationic nature which may increase cellular uptake (with amino groups which could be ionized at acidic pH in the tumor environment).

Based on the above, the aim of this study was to prepare mixed micelles of LACPEG and DSPE-PEG and to analyse their efficacy in preclinical *in vitro* and *in vivo* studies for the delivery of a hydrophobic anticancer drug. A prototype EGFR tyrosine kinase inhibitor with the following characteristics was selected; molecular weight (Mw <1 kDa), sparingly soluble or practically insoluble across the physiological pH range and Log P: 4.85. This is the first study which investigates the use of this novel polymer, LACPEG, with DSPE-PEG for the delivery of a hydrophobic anticancer drug.

2. Materials and methods

2.1 Materials

The hydrophobic drug used is AstraZeneca proprietary (Log *P:* 4.85, pKa: 5.42 and 7.24). Chitosan oligosaccharide (Mw 3-5 kDa, degree of deacetylation, > 90%, Kittolife Co., Seoul, Korea), 1,2-distearoyl-sn-glycero-3-phosphatidylethanolamine-n-methoxy(polyethylene glycol)-2000 (DSPE-PEG, Mw 2 kDa, Lipoid GmBH, Germany) were used in this study. The following reagents, solvents and solutions were obtained from Sigma Aldrich (USA): poly(vinyl alcohol) (PVA, Mw 13-23 kDa, 87-89% hydrolyzed), lipoic acid, *N*-hydroxysuccinimide (NHS, 98%), dichloromethane (DCM, > 99.8%, anhydrous), dimethylsulfoxide (DMSO, anhydrous, > 99.9%), sodium acetate, RPMI-1640, L-glutamine 200 mM, 100x antibiotic-antimycotic solution, Dulbecco's phosphate buffered saline (DPBS) and Triton X-100. The following materials were purchased from Fisher (UK): sodium hydroxide, acetonitrile (ACN, HPLC grade) and ethyl acetate. The following materials were also used: *N, N*-dicyclohexylcarbodiimide (DCC, Alfa Aesar, USA), methoxy-PEG-*N*-hydroxy succinimide

(mPEG-NHS, Mw 5.4 kDa, Advanced Polymer Materials, Canada), Opti-MEM® and TrypLE express and foetal bovine serum (FBS) (Gibco Invitrogen, USA), 3-(4,5-dimethylthiazol-2-yl)-5-(3-carboxymethoxyphenyl)-2-(4-sulfophenyl)-2H-tetrazolium compound (MTS) and phenazine methosulfate (PMS) (CellTiter 96® Aqueous One Solution Cell Proliferation Assay, Promega, USA) and PLGA (DL-lactide/glycolide ratio 85:15, Mw 149 kDa, Alkermes Medisorb, USA). Live/Dead® BacLight viability kit containing propidium iodide and Syto 9 dye was purchased from Life Technologies Corporation, USA. The following materials were purchased for *in vivo* studies: Advanced RPMI-1640 media, penicillin-streptomycin 100x, Trypsin-EDTA (1x) with phenol red Glutamax™ supplement, phosphate buffered saline PBS (10x and 1x, pH 7.4) were obtained from Gibco, Invitrogen (UK), plasma derived bovine serum (FBS) (First-Link, UK), pentobarbital sodium (Euthatal®, Merial, UK), Dulbecco's Modified Eagle Medium (DMEM, Invitrogen, USA) and carbocyanine perchlorate dye (DiI, Santa Cruz Biotechnology, USA). HPLC grade deionised water was used throughout, unless otherwise stated.

2.2 Synthesis of LACPEG

1 g lipoic acid (4.85 mmol) was dissolved in 20 mL DCM and reacted with NHS (560 mg, 4.87 mmol) and DCC (820 mg, 3.97 mmol), each dissolved in 10 mL of DCM. This reaction was carried out in the dark, under nitrogen at room temperature for 48 h. The solution was filtered (Whatman filter paper, 150 mm) to remove dicyclohexylurea crystals and rotary evaporated at 60°C and 280 rpm (Heidolph, UK) to remove solvent. The resultant thin film was dissolved in 20 mL anhydrous DMSO. 1 g mPEG-NHS (0.19 mmol) dissolved in 10 mL anhydrous DMSO was added to this solution, followed by addition of chitosan oligosaccharide (3-5 kDa) solution (23.26 mmol), prepared by dissolving 4 g chitosan oligosaccharide in 10 mL anhydrous DMSO and 5 mL water. The solution was stirred, under nitrogen, in the dark, for 48 h. This was filtered and dialysed (molecular weight cut-off, MWCO; 7 kDa) against DMSO for 2 h and water for a further 4 days. The resultant solution was lyophilised (Benchtop 2.0, Virtis Advantage, UK) to produce LACPEG. Lyophilisation (32 h) involved freezing the samples (-60°C), followed by primary and secondary drying, in which the vacuum (200 mT) was applied and the shelf temperature gradually increased to -20°C and then to +20°C.

2.3 Confirmation of LACPEG synthesis

2.3.1 Fourier transform-infrared (FT-IR) spectroscopy

2 mg of lyophilised polymer and raw materials (chitosan, lipoic acid and mPEG-NHS) were analysed using a Perkin-Elmer Spectrum 100 Fourier transform infrared (FT-IR) spectrometer (Perkin-Elmer, USA). FT-IR spectra were obtained in the range of 400-4000 cm^{-1} at a resolution of 4 cm^{-1} and analyzed using Perkin-Elmer Express software (Perkin Elmer, USA).

2.3.2 Proton nuclear magnetic resonance (^{1}H NMR) spectroscopy

5 mg chitosan was dissolved in 0.6 mL deuterium oxide, and 5 mg of lipoic acid and LACPEG were dissolved in 0.6 mL of deuterated chloroform and analyzed using a 400 MHz NMR spectrometer equipped with a ^{1}H inverse probe (Bruker Avance, Germany), and spectra processed using ACD/labs software (v. 12.01, Advanced Chemistry Development, UK).

2.4 Preparation of hydrophobic drug-loaded micelles

Mixed micelles of LACPEG and DSPE-PEG were prepared using an optimized in-house method. Briefly, 10 mg of LACPEG, DSPE-PEG and a 50:50 mixture of the two polymers (with and without 0.5 mg hydrophobic drug) were dissolved in 5 mL ACN. The polymer to drug ratio was selected based on preliminary studies (results not shown) as the optimum ratio with the highest drug entrapment efficiency. ACN was removed using a rotary evaporator (Hei-VAP Advantage Rotary Evaporator, Heidolph, Germany) at 85°C, 150 rpm and 0 bar pressure (KNF Laboport, KNF Neuberger, Germany) for 15 min. The resultant thin film was dried under nitrogen to remove residual solvent. 1.5 mL of acetate buffer pH 4.1 (preheated at 55°C) was added to this film and mixed continuously in a 55°C water bath (Buchi B480, Sweden) for 5 min. A pH of 4.1 was employed to enhance drug solubility and increase the positive charge of polymer to maximise drug-polymer interaction and drug entrapment. The solution was then bath sonicated (Ultrawave bath sonicator, Ultrawave, UK) for 10 min, and allowed to stand for 3 h. The final solution was neutralized with sodium hydroxide, to be compatible with *in vitro* cell studies and filtered through a 0.22 µm filter (Millex-MP, Millipore, Ireland) to remove unentrapped drug. This preparation was used for the remaining studies.

For *in vivo* distribution and imaging studies micelles were prepared as described, with 375 µg DiI (2 mg/mL) replacing the hydrophobic drug. Samples were filtered using a PD-10 desalting column (GE

Healthcare Life Sciences, UK) and then concentrated using centrifugal concentrators (Vivaspin 10 kDa, Vivascience, Germany) at 4°C, 4450 rpm for 45 min (Centrifuge 5804R, Eppendorf, Germany). PLGA microparticles, with a mean size 3.70 µm, were prepared using the w/o/w double emulsion method (Lee et al., 2013). These microparticles are rapidly cleared from the blood and accumulate in the liver and spleen because of their large size (Lecaroz et al., 2007). Therefore, they were selected as negative controls for the micelles prepared in this study, which are hypothesized to reach the tumor and show minimal spleen and liver accumulation.

2.5 Nanocarrier size distribution and surface charge

Nanocarrier size and surface charge were analyzed using dynamic light scattering and laser Doppler velocimetry, respectively (Zetasizer, Malvern Nano ZS, Malvern Instruments, UK). The kinetic stability of empty and hydrophobic drug-loaded micelles was assessed by measuring changes in particle size over time (Ribeiro et al., 2012). Briefly, samples were placed in air-tight containers at 25°C and analyzed for their particle size distribution on the day of the preparation (day 0) and at various time intervals over 30 days.

2.6 Nanocarrier morphology

The morphology of empty and hydrophobic-loaded micelles was assessed using transmission electron microscopy (TEM). 20 µL of sample was negatively stained with 1% uranyl acetate on a nitrocellulose-covered copper grid and observed using an FEI CM 120 Bio Twin transmission electron microscope (Philips Electron Optics, Netherlands). Images were taken using AMT digital TEM camera software (Deben UK, UK).

2.7 *Solid-state properties*

2.7.1 Differential scanning calorimetry (DSC)

The solid-state properties of the polymers and lyophilised micelle preparations were assessed using pin-hole differential scanning calorimetry (DSC Q2000 module, TA Instruments, LLC, USA), as previously described (Slager and Prozonic, 2005). 5 mg samples were crimped in aluminium pans (TA Instruments, LLC, USA) and heated at a rate of 20°C/min from 20 to 200°C (chitosan was heated to 350°C), cooled to -20°C and then heated back up to 200°C under nitrogen atmosphere at a flow

rate of 50 mL/min to prevent oxidation. An empty aluminium pan was used as a reference and indium used to calibrate the instrument. The thermograms where drawn using Universal Analysis 2000 software (TA Instruments, LLC, USA).

2.7.2 X-ray powder diffraction studies (XRPD)

Solid-state properties were further assessed using X-ray powder diffractograms obtained from a Cu Kα radiation-based diffractometer (Xcalibur novaT X-ray diffractometer, Oxford Diffraction, Oxford, UK), which were processed using CrysalisPro software (Oxford Diffraction, Oxford, UK) and scanned at a step size of 10°2-theta.

2.8 Hydrophobic drug loading and entrapment efficiency

Reversed-phase high performance liquid chromatography (RP-HPLC) was used to quantify drug loading (DL) and entrapment efficiencies (EE). HPLC equipment was obtained from Agilent Technologies (UK); G1311C Quaternary Pump, G1329B Automatic Liquid Sampler and G1314C Variable Wavelength Detector. A Zorbax Eclipse® Plus C18 column (4.6 x 100 mm x 3.5 µm) was used with a guard cartridge (Fast Guard, 1.8 µm, Eclipse Plus C18, 4.6 mm). An isocratic mobile phase comprised: ammonium acetate (0.6 % w/v), ACN (38 % v/v) and MilliQ water (62 % v/v). RP-HPLC was run with a flow rate of 1 mL/min, column temperature of 60°C, injection volume 2 µL and runtime 30 min. The lowest limit of quantification and the lowest limit of detection for the hydrophobic drug were 31 and 7.8 µg/mL, respectively. DL and EE were calculated using the following equations (Elsaid et al., 2012):

$$DL\ (\%) = \frac{\text{Amount of drug}}{\text{Amount of polymer + drug}} \times 100 \quad (1)$$

$$EE\ (\%) = \frac{\text{Measured drug loading}}{\text{Theoretical drug loading}} \times 100 \quad (2)$$

2.9 Cell culture viability assays

A549 and PC-9 cells (European Collection of Cell Cultures) were cultured in RPMI-1640 supplemented with 10% FBS, 1x antibiotic-antimycotic and 1% L-glutamine at 37°C in a humidified incubator with 5% CO_2.

2.9.1 MTS assay

The effect of drug solution, empty and drug-loaded micelles on the viability of A549 and PC-9 cells was investigated. Briefly, the MTS assay (CellTiter 96® Aqueous One Solution Cell Proliferation Assay, Promega, USA) was conducted in accordance with the manufacturer's instructions. Cells were seeded at a density of 2000 cells/well in 96-well plates and allowed to attach for 24 h. A549 and PC-9 cells were then exposed to samples for 72 h. MTS (5 mg/mL in PBS with PMS) was then added to the wells and incubated for a further 2 h, after which a water-soluble formazan product was produced, and absorbance measured at 490 nm using a microplate reader (Synergy HT, Bio-Tek Instruments, USA). The range of concentrations of micelles used in the drug-loaded micelles was equivalent to that used with the empty micelles, allowing direct comparison and determination of the effect of both micelles and drug on cell viability. Cell viability was expressed relative to control cells; with those exposed to media alone and those exposed to 1% Triton-X acting as positive and negative controls, respectively. Graphs were drawn using OriginPro 9.0. IC_{50} values were taken as the concentration that would result in 50% cell viability.

2.9.2 Live/Dead assay

A549 and PC-9 cells were prepared as for the MTS assay and exposed to media, 1% Triton-X or sample solutions for 72 h. The samples containing drug were prepared at concentrations of 10 and 0.4 µM for A549 and PC-9 cells respectively, with empty micelles prepared at equivalent concentrations. Cells were exposed to a solution comprising Syto 9 (3.34 µM) and propidium iodide (PI, 7.48 µM) and the cell viability and morphology imaged using a fluorescence microscope (EVOS® FL Auto Imaging System, Life Technologies, USA).

2.10 In vivo assessment

2.10.1. Animal model

Animal studies were conducted in accordance with the UK Home Office Code of Practice and EU Directive 2010/63/EU for the Housing and Care of Animals used in Scientific Procedures. Female 4-6

week old BALB/c mice (Harlan, UK) were subcutaneously inoculated with $1x10^6$ (in 20 µL) CT26 colon cancer cells bifocally in the hind foot. Tumors reached a size of 500 mm^3 by day 12, after which the mice were injected with the formulations. For comparative purposes, 4-6 week old female C57/BL6 mice (Harlan, UK) were inoculated bifocally with $1x10^6$ (in 100 µL) LLC cells/site (in the lower flank) and tumors grown to a size of 300 mm^3.

Prior to subcutaneous inoculation, CT26 (CRL-2638, ATCC) and LLC cells (CRL-1642, ATCC) were cultivated in RPMI-1640 and DMEM, respectively, supplemented with 10% FBS, 1% L-glutamine and 100 IU/mL penicillin/streptomycin.

2.10.2 In vivo and ex vivo biodistribution determined by optical imaging

DiI-loaded micelles were injected into mice tail veins, at a dose of 500 mg/kg (DiI loading varied between formulations, range: 62-100%), and the mice imaged at different times (5 min, 1 h, 4 h and 24 h) using a pre-warmed (37°C) IVIS® Lumina series III imaging device (Caliper Life Sciences, Perkin Elmer, USA). Treatment groups (n=3) included: control mice (injected with PBS), negative control (DiI-loaded PLGA microspheres), treatment mice (DiI-loaded DSPE-PEG and LACPEG/DSPE-PEG micelles). 24 h post-injection, mice were sacrificed by cervical dislocation and their major organs (heart, lungs, liver, spleen, intestine and kidneys) and tumors excised for *ex vivo* imaging. Fluorescence images were obtained using excitation wavelengths of 480, 500, 520, 540 and 560 nm and emission wavelength of 610 nm, with exposure time: 3 s; binning factor: 4; f number 2 and field of view: E-25 cm. Images were processed using the Living Image 4.3.1 service pack 2 software (Caliper Life Sciences, Perkin Elmer, USA). The fluorescence intensities quantified were divided by the weight of each organ and normalised to the liver, to account for variations in tissue weight and DiI dose injected, respectively.

2.10.3 Flow cytometry analysis of ex vivo tumor cells

Tumors were dissected, homogenized and trypsinized to obtain a single cell suspension which was analysed by fluorescence-activated cell sorting (FACS) using a flow cytometer (FACSCalibur BD Biosciences, USA) and CellQuest software (Becton Dickinson, USA). DiI was measured with a FL-4 channel and data obtained from at least 5 x 10^4 cells. Autofluorescence from untreated cells was

subtracted from the fluorescence of treated cells. Results were expressed as fluorescence intensity ± SD (n=3).

2.11 Statistical Analysis

Data were analysed using two-way analysis of variance and unpaired two-tailed student's *t* test, with a *p* value of < 0.05 considered as significant.

3. Results

3.1 Confirmation of LACPEG synthesis-FT-IR and ^{1}H NMR spectroscopy

The FT-IR spectrum for LACPEG (Fig. 1A) shows peaks at 842, 961, 2884 and 1060-1150 cm^{-1} which correspond to the mPEG component of the structure. The broad peak at 3070-3621 cm^{-1} represents the hydroxyl and amino groups of chitosan. The C-O and C=O vibrations (1250 and 1680 cm^{-1}, respectively) of lipoic acid reduced with the grafted sample. A new peak occurred at 1648 cm^{-1} representing amide-bond formation. These peaks confirm successful synthesis of LACPEG.

Fig. 1B shows ^{1}H NMR spectra for LACPEG, chitosan and lipoic acid. The spectrum for chitosan showed peaks for the methyl, ethyl and sugar protons of the structure between 1.81 and 4.54 ppm. Peaks corresponding to these protons (1.65-4.16 ppm) were also obtained in the ^{1}H NMR spectrum of LACPEG. The peaks between 1.34 and 3.53 ppm and the peak at 3.62 ppm correspond to the lipoic acid and PEG components of LACPEG copolymer, respectively. Thus, synthesis of LACPEG was confirmed, supporting the FT-IR data.

Fig. 1. FT-IR spectra for lipoic acid, chitosan, mPEG-NHS and LACPEG (A). ^{1}H NMR spectra for chitosan in D_2O, lipoic acid in $CDCL_3$ and LACPEG in $CDCL_3$ (B). The spectrum for LACPEG contains peaks from the separate components, with an additional peak representing amide bond formation. Grey line represents water content present in chitosan. These spectra confirm LACPEG synthesis. Abbreviations: D_2O: deuterium oxide and $CDCL_3$: deuterated chloroform.

3.2 Size and surface charge

The size, PDI and surface charge of empty and drug-loaded micelles are shown in Table 1. The mean size of empty micelles was: LACPEG: 130 ± 1.25 nm, DSPE-PEG: 30.1 ± 0.39 nm, LACPEG/DSPE-PEG: 100 ± 0.62 nm. The mean size of these micelles was reduced significantly with the addition of the drug. LACPEG and LACPEG/DSPE-PEG micelles were positively charged and DSPE-PEG micelles were negatively charged. The surface charge became more positive/less negative on loading with the positively charged hydrophobic drug.

The physical stability of the micelles was assessed with respect to size distribution over 30 days period (Fig. 2). Empty DSPE-PEG micelles increased 13-fold in mean size by day 30 ($p<0.05$); PDI also increased from 0.5 on the day of preparation to 0.9 on day 30. LACPEG and LACPEG/DSPE-PEG micelles had a consistent mean size throughout the 30-day period, with unchanged PDI vales of 0.2 and 0.5 for LACPEG and LACPEG/DSPE-PEG micelles, respectively. The size distribution was unchanged over 30 days for all hydrophobic drug-loaded micelles.

Fig. 2. Hydrodynamic diameters of empty and drug-loaded micelles. Micelles maintained their size throughout the 30 day period, with the exception to DSPE-PEG micelles, which showed aggregation at day 30 (*$p<0.01$). The use of LACPEG or entrapment of the hydrophobic drug improved micelle stability. Abbreviations: H: hydrophobic drug, L: LACPEG, L/D: LACPEG/DSPE-PEG and D: DSPE-PEG. Results are expressed as mean ± SD (n=3).

3.3 Morphology

Fig. 3 shows the morphology of the empty and drug-loaded micelles as observed under TEM. DSPE-PEG micelles were clear structures and appeared larger than the LACPEG micelles. Micelles of LACPEG/DSPE-PEG differed in morphology to DSPE-PEG and LACPEG micelles.

Fig. 3. Transmission electron micrographs of micelles. Abbreviation: H: hydrophobic drug.

3.4 Solid-state properties

3.4.1 DSC

Fig. 4 A shows the thermograms for the synthesized LACPEG polymer and its native constituents (lipoic acid, chitosan and PEG). The thermogram for chitosan showed a broad endothermic peak at 100°C secondary to water loss. The single endothermic peak at 64.2°C signifies the melting temperature of lipoic acid. PEG showed a bifurcated peak at 53.3°C and 57.6°C representing the presence of two polymorphic forms. The synthesized LACPEG polymer had a similar bifurcated peak to PEG but at lower temperatures of 48.9°C and 54.6°C.

The thermograms for the empty and drug-loaded micelles are shown in Fig. 4 B. The hydrophobic drug showed a single endothermic peak at 194.1°C which reflects its crystalline nature. This peak disappeared in the thermograms for all of the drug-loaded micelles. The empty LACPEG micelles had a similar bifurcated peak as for the synthesized polymer, but at lower temperatures of 47.1°C and 51.5°C. This became a single endothermic peak with a higher melting temperature of 56.4°C with drug entrapment. A similar effect was obtained for the LACPEG/DSPE-PEG micelles. These micelles had a melting temperature of 55.2°C which was very similar to DSPE-PEG micelles. However, unlike LACPEG and LACPEG/DSPE-PEG micelles, the melting temperature of the DSPE-PEG micelles (55.1°C) did not differ with drug entrapment or to the native polymer.

3.4.2 XRPD

Fig. 4 C shows the diffractograms for the LACPEG polymer and its native constituents. Lipoic acid is predominately crystalline, as demonstrated by several sharp peaks at 2θ = 18.5°, 22° and 24°. PEG showed semi-crystalline properties with characteristic peaks at 2θ = 19° and 23°. Chitosan showed broad diffraction peaks at 2θ = 18°, 33° and 40°. The diffractogram for LACPEG showed the characteristic peaks of PEG and chitosan at 2θ = 19°, 23° and 33°. The diffraction pattern of lipoic acid was reduced in LACPEG.

Fig. 4 D shows the diffractograms for empty and drug-loaded LACPEG and DSPE-PEG micelles. The hydrophobic drug showed crystalline properties with several characteristic peaks at 2θ = 19°, 24° and 26°. These peaks, except for 2θ = 24°, were absent in the diffractograms for the drug-loaded micelles. This decline in crystallinity further confirms the DSC findings and may be attributed to drug entrapment. The DSPE-PEG polymer showed semi-crystalline properties with peaks at 2θ = 19°, 22°,

24° and 26°. The peaks for the DSPE-PEG polymer, together with those of LACPEG polymer, were all present in their respective micelles indicating that all of the micelles retained the semi-crystalline properties of their polymers.

Fig. 4. DSC thermograms for chitosan, lipoic acid, poly(ethylene glycol) and LACPEG (A). LACPEG had similar thermal properties to its native constituents (chitosan, PEG and lipoic acid), showing a bifurcated peak and a broad water loss peak. DSC thermograms for empty and hydrophobic drug-loaded LACPEG and DSPEPEG micelles and their native constituents (B). The thermogram for the hydrophobic drug had a single endothermic peak at 194.1°C. Empty and drug-loaded micelles had melting temperatures in the range of 47.1°C - 56.4°C. Drug entrapment resulted in the formation of micelles with a more thermally-stable polymorphic form. XRPD diffractograms for chitosan, lipoic acid, PEG and LACPEG (C). PEG and lipoic acid showed crystalline properties. Chitosan and LACPEG had semi-crystalline properties. XRPD diffractograms for empty and drug-loaded micelles and their native constituents (D). Micelles showed semi-crystalline properties. Abbreviations: PEG: poly(ethylene glycol); LACPEG: lipoic acid-chitosan-poly(ethylene glycol); L: LACPEG, D: DSPE-PEG and H: hydrophobic drug.

3.5 Hydrophobic drug loading and entrapment efficiency

Micelle DLs and EEs are shown in Table 2. DSPE PEG micelles showed no significant difference in EE compared to LACPEG/DSPE-PEG, though LACPEG micelles showed a significantly lower EE ($p<0.05$).

3.6 Cell culture viability assays

3.6.1 MTS assay

Fig. 5 shows the effect of drug solution, empty and drug-loaded micelles on the viability of A549 and PC-9 cells. The empty micelles (Figs. 5 A and B) produced a cell-specific reduction in viability. For example, 1 mg/mL of DSPE-PEG micelles showed 80% cell viability in A549 cells (Fig. 5 A) and a much lower viability of 1.92% in PC-9 cells (Fig. 5 B). The mechanisms behind this need to be further studied. The cytotoxic effects elicited by the empty micelles, for both cell lines, were in the order: LACPEG > DSPE-PEG > LACPEG/DSPE-PEG.

The drug had IC_{50} values of 11.9 ± 0.81 μM and 0.19 ± 0.15 μM in A549 and PC-9 cells, respectively, denoting drug-refractory and sensitive cell lines, respectively (Fig. 5 C and D). Hydrophobic drug-loaded LACPEG micelles increased the sensitivity of A549 cells, with an IC_{50} 1.7-fold lower than drug alone (6.85 ± 1.85 μM compared to 11.9 ± 0.81 μM; p<0.001), unlike drug-loaded DSPE-PEG and LACPEG/DSPE-PEG micelles ($IC_{50:}$ 14.5 ± 2.75 μM and 9.90 ± 2.29 μM, respectively; p>0.05). The toxicity of drug-loaded micelles in A549 cells was in the order: LACPEG > LACPEG/DSPE-PEG> DSPE-PEG and for PC-9 cells: DSPE-PEG > LACPEG > LACPEG/DSPE-PEG (IC_{50} values of 0.10 ± 0.01, 0.24 ± 0.18 and 0.30 ± 0.13 μM, respectively).

Fig. 5. Viability for A549 and PC-9 cells exposed to empty micelles (A and B), drug alone and drug-loaded micelles (C and D) at concentrations indicated for 72 h. The concentration of micelles in the drug-loaded micelles (Fig. 5 C and D) was equivalent to the range used in the empty micelles (Fig. 4 5 and B). Empty micelles showed a reduction in the viability of both cell lines in the order of LACPEG> DSPE-PEG> LACPEG/DSPE-PEG. Greater cell death was obtained with drug-loaded LACPEG micelles compared to drug-loaded DSPE-PEG and LACPEG/DSPE-PEG micelles, as empty LACPEG micelles showed the greatest toxicity and this contributed to the toxicity observed with the drug-loaded micelles. All of the tested formulations caused greater cell death in PC-9 cells compared to A549 cells. Abbreviations: L: lipoic acid-chitosan-poly(ethylene glycol); D: DSPE-PEG and H: hydrophobic drug. Results are expressed as mean ± SD (n=9).

3.6.2 Live/Dead assay

The Live/Dead assay was conducted on A549 (Fig. 6 A) and PC-9 (Fig. 6 B) cells to analyze the effects of drug solution, empty and drug-loaded micelles on cell viability and morphology. SYTO 9 permeates intact cell membranes of viable cells and stains the nuclei, emitting green fluorescence, whereas, PI stains dead cells with disrupted membranes and emits red fluorescence. The findings from this assay confirmed those obtained with the MTS assay, showing a similar proportion of dead cells. The drug induces apoptosis (Fig. 6). The entrapment of drug in all the micelles studied resulted in a greater proportion of dead cells compared to drug solution and empty micelles; an effect most pronounced with drug-loaded LACPEG in A549 cells and with drug-loaded LACPEG, DSPE-PEG and LACPEG/DSPE-PEG micelles for PC9 cells. Effects were greater for PC-9 cells (Fig. 6 B) compared

to A549 cells (Fig. 6 A), as the former are mutant EGFR cells and are therefore more sensitive to EGFR TKIs.

Fig. 6. Live-dead fluorescence images of A549 (A) and PC-9 (B) cells, exposed to drug solution, empty and drug-loaded micelles for 72 h. Controls used in this study were media-treated (positive) and Triton-X-treated (negative) cells. Abbreviation: H: hydrophobic drug. The images depict a greater proportion of dead (stained red with propidium iodide) compared to living (stained green with SYTO 9) cells for the drug-loaded micelles compared to the empty micelles and drug solution.

3.7 In vivo and ex vivo assessment

3.7.1 In vivo and ex vivo biodistribution determined by optical imaging

DiI-incorporated DSPE-PEG and LACPEG/DSPE-PEG micelles showed prolonged whole body circulation half-life (high fluorescence signals over 24 h following injection) and higher tumor accumulation compared to the negative control (PLGA microparticles) which exhibited lower whole body signals and higher signals in the liver and spleen (Fig. 7), due to short blood circulation time and high RES uptake *in vivo.* These results were confirmed with the *ex vivo* studies carried out after 24 h (Fig. 7 B). The fluorescence intensities quantified were divided by the weight of each organ and normalised to the liver, to account for variations in tissue weight and DiI dose injected, respectively, (Fig. 7C) and showed that there was no significant difference in tumor accumulation between DSPE-PEG and LACPEG/DSPE-PEG micelles, although they both showed 20-40-hold higher fluorescence (hence tumor accumulation) than PLGA microparticles. Prolonged circulation half-lives and tumor accumulation over 24 h for DSPE-PEG and LACPEG/DSPE-PEG micelles were also seen in *in vivo* and *ex vivo* studies conducted in LLC-tumor bearing C57/BL6 mice (Fig. 7 D-E).

Fig. 7. *In vivo* bioluminescence imaging of DiI-incorporated micelles in CT-26 tumor-bearing BALB/c mice (A). Mice were intravenously injected (500 mg/kg dose, DiI dose administered varied with entrapment efficiency) into the tail vein and whole body dorsal and ventral images taken over a 24 hour period (white arrows signify tumors). Control mice were injected with PBS solution. Prolonged whole body circulation and tumor accumulation was obtained for the micelles compared to the PLGA microparticles (negative control), which showed higher signals in the liver and spleen. *Ex vivo* bioluminescence studies for DiI-incorporated micelles in CT-26 tumor-bearing BALB/c mice images (B) and quantification of fluorescence signals for excised organs and tumors at 24 h, normalised to the liver (C), confirmed *in vivo* results. *In vivo* (D) and *Ex vivo* (E) bioluminescence imaging of DiI-incorporated micelles in LLC tumor-bearing C57/BL6 mice. All images were obtained by IVIS Lumina® III at exposure time: 3 s; binning factor: 4; f number 2, field of view: E-25 cm; λex: 480, 500, 520, 540 and 560 nm; λem: 620 nm. Results are expressed as mean ± SD (n=3) for A, B and C and n=1 for D and E. Abbreviations: D: DSPE-PEG and L/D: LACPEG/DSPE-PEG.

3.7.2 Flow cytometric analysis for tumor uptake

FACS was performed to examine cellular internalization of DiI-incorporated DSPE-PEG and LACPEG/DSPE-PEG micelles (Fig. 8). Mean fluorescence was approximately 10 to 12 X higher than control (PBS solution) for DSPE-PEG and LACPEG/DSPE-PEG micelles (p<0.05), respectively, but did not differ from each other (p=0.05). It should be noted that a smaller amount of dye was injected into the mice in the case of LACPEG/DSPE-PEG compared to DSPE-PEG, due to differences in initial dye loading (63% and 100% DiI loading 100%, respectively), indirectly suggests that LACPEG/DSPE-PEG is able to internalise more efficiently into tumor cells than DSPE-PEG.

Fig. 8. Flow cytometric analysis of tumor uptake for DiI-incorporated micelles in CT26 tumor-bearing BALB/c mice. Histograms (A) and percentage (B) of DiI-positive tumor cells for each formulation are depicted. An FL-4 laser was used to analyse the tumor cells 24 h after micelle administration. Control mice were injected with PBS solution. DSPE-PEG and LACPEG/DSPE-PEG micelles showed a higher percentage of DiI-positive tumor cells compared to the control (p<0.05) but not from each other (p=0.05). Results are expressed as mean ± SD (n=3).

4. Discussion

Mixed micelles of LACPEG and DSPE-PEG were studied with the aim of improving the loading and delivery of a hydrophobic anticancer drug, with the chitosan component contributing to the cationic nature of the carrier, and the DSPE-PEG and lipoic acid components increasing circulation half-life, carrier stability and cellular uptake, as well as reducing carrier toxicity.

The conjugation of lipoic acid and PEG components, to the amino groups of chitosan, were confirmed using FT-IR and 1H NMR (Fig. 1). Hydrophobic drug-loaded micelles of LACPEG, DSPE-PEG and LACPEG/DSPE-PEG were prepared and characterized. As in Fig. 2, LACPEG micelles had mean size 130 nm, which corresponds with studies of pluronic-chitosan and stearic acid-chitosan micelles, which reported sizes of 93-181 and 33-131 nm, respectively (Lin and Chang, 2013; Yuan et al., 2011). The positive surface charge of these micelles (+3.95 ± 1.03 mV; Table 1) is likely to be attributable to the chitosan component; previous studies have reported a concentration-dependent increase in the cationic nature of carriers based on the protonation of free surface amino groups of chitosan, in low pH environments. DSPE-PEG micelles were 30 nm in size, agreeing closely with published data (Remsberg et al., 2012). The combination of LACPEG and DSPE-PEG polymers resulted in micelles of significantly (p<0.001) smaller mean size compared to LACPEG micelles (100 and 130 nm, respectively). DLS results showed a single peak for the LACPEG/DSPE-PEG mixed micelles with an average PDI value of 0.35, indicating a fairly monodisperse pattern of size distribution. Similar PDI values have been noted with previous mixed micelles, in literature (Kulthe et al., 2014; Pepic et al., 2014; Varshosaz et al., 2015). Although drug loading did result in an increase in the PDI value to 0.57, this was similar to the PDI value of DSPE-PEG micelles (0.52 and 0.44 for empty and drug-loaded, respectively).

Drug loading in LACPEG/DSPE-PEG micelles halved the size of the micelles (p<0.001), an affect which was not observed for the LACPEG or DSPE-PEG micelles. This condensation may be attributed to differences in drug-micelle core interactions (Lee et al., 2004). In the case of LACPEG/DSPE-PEG there could be increased strength in the cohesive forces between the drug and micelle core because of the increased hydrophobicity of the mixed micelles (with the additional lipoic acid component), which would also increase the stability of the micellar core (Tian and Mao, 2012), and correlates with the increased physical stability (Fig. 2) and thermodynamic stability (Fig. 4) of

these mixed micelles, discussed below. Furthermore, there are greater London dispersive forces within the mixed micelles, which could also contribute to the dramatic reduction in size of the micelles with drug entrapment. This is because the London dispersive force between the hydrophobic drug and the hydrophobic blocks within the polymer is stronger than that between the hydrophobic drug and water (Kim et al., 2010), and is stronger than that which exists in the single micelles given the greater hydrophobic content of the mixed micelles. This dramatic reduction in micelle size is carrier specific, as in the literature, either no visible effect (Chen et al., 2013) or an increase (Ebrahim Attia et al., 2011; Zhao et al., 2012) in particle size and distribution was noted for other mixed micelles after hydrophobic drug loading. This is a major advantage to the use of these mixed micelles, given that the smaller size may aid tumor accumulation and cellular uptake. The difference in the interaction between the drug and the mixed micelles and the single micelles is further confirmed with the zeta potential values (Table 1), where an increase in positive charge was noted with drug entrapment for LACPEG and DSPE-PEG micelles and a reduction in positive charge observed for drug-loaded LACPEG/DSPE-PEG micelles. It could be inferred from this finding that the difference in interactions (hydrophobic and London dispersive forces) for the mixed micelles influences the arrangement of the polymer and hence its surface charge.

Empty DSPE-PEG micelles increased dramatically in mean size ($p<0.01$), with increased polydispersity by day 30, indicating reduced physical stability and aggregation. Previous studies have demonstrated that storage of these micelle solutions for longer than a week at 25°C results in carrier instability and precipitate formation (Johnsson et al., 2001). LACPEG and LACPEG/DSPE-PEG micelles had consistent size distribution over the test period, suggesting a stability-enhancing influence from the LACPEG. Improved stability may have been achieved by variations in the hydrophobic (lipoic acid and DSPE) and hydrophilic components (PEG and chitosan) of the micelles; their chain length, molecular weight or content (Adams and Kwon, 2003). Improved stability has previously been associated with mixed PEG-based micelles, such as poly(histidine)-PEG/DSPE-PEG and PEG-DSPE/TPGS (Wang et al., 2014; Wu et al., 2013). Increased storage stability of mixed micelles has been attributed to the increased interactions between the hydrophobic chains in the micellar core which would stabilize the structure, or to specific polymer characteristics, such as PEG content (Gao et al., 2008; Li et al., 2011; Zheng et al., 2016). Drug-loading increased DSPE-PEG

micelle stability (Fig. 2). This agrees with previous studies, which demonstrated that nanocarrier stability is influenced by hydrophobic drug-micelle core interactions (Lee et al., 2004).

When observed using TEM (Fig. 3), DSPE-PEG micelles appeared similar in structure to previously reported (Zhao, 2013) micelles. Micelles of LACPEG/DSPE-PEG differed in morphology to DSPE-PEG and LACPEG micelles, confirming the production of a new carrier.

The solid-state properties for the empty and drug-loaded micelles were also assessed using DSC and XRD (Fig. 4). The thermogram for chitosan was similar to that reported by other studies (Duan et al., 2004; Elsaid et al., 2012). The same was also true for the lipoic acid thermogram (Zhao et al., 2014). The reduction in the melting temperature of PEG, in the thermogram for LACPEG, indicates that the crystallization of this polymer was affected, possibly due to the chemical conjugation of PEG to the backbone of chitosan (Duan et al., 2004; Huang et al., 2010). The water loss from chitosan, seen at 100°C was present in the thermogram for LACPEG. These results further corroborate the conjugation of the components to the chitosan backbone as was seen with the FT-IR and 1H NMR data (Fig. 1). The results obtained with XRD confirmed those found with the DSC data. The diffractograms for lipoic acid (Zhang et al., 2013), PEG (Elsaid et al., 2012) and chitosan (Kumirska et al., 2010) correlated with literature. The peaks pertaining to lipoic acid within the LACPEG diffractogram reduced showing a decline in crystallinity which was in line with the DSC findings.

The melting point peak for the drug was not seen with the thermograms of the drug-loaded micelles, indicating a decline in the drug's crystallinity, possibly due to drug entrapment (Nasr et al., 2008; Tursilli et al., 2006). Although the formation of the LACPEG micelles resulted in a reduction in the thermal stability when compared to the LACPEG polymer (as seen by a reduction in the melting points of the bifurcated peak), upon drug-entrapment a higher melting was seen, indicating the formation of a more thermally-stable polymorphic form of LACPEG micelles. The same was also seen with the LACPEG/DSPE-PEG, perhaps indicating a greater influence of the LACPEG component than the DSPE-PEG component on the thermal properties of the micelles. The melting point of DSPE-PEG micelles, unlike LACPEG/DSPE-PEG and LACPEG micelles, did not differ with drug-entrapment. Thus, gefiinib-entrapped LACPEG and LACPEG/DSPE-PEG micelles were more

thermally stable than DSPE-PEG micelles (Fig. 4), further confirming the physical stability data obtained (Fig. 2). Furthermore, drug loading in the DSPE-PEG micelles caused an increase in the width of the endothermic peak (Fig. 4). This may have been caused by PEG chain-chain entanglement as a result of van der Waals forces reported in PEG-based lipids (Hashizaki et al., 2003) and interaction with the hydrophobic drug.

The EE of LACPEG micelles was 45.6% (Table 2). A study of nanocarriers prepared from amphiphilic derivatives of chitosan, loaded with hydrophobic drugs (e.g. paclitaxel), reported EEs in the range of 23-32% (Aranaz, 2010). This low EE may be due to the presence of multiple hydrophilic components, chitosan and PEG, which reduce the solubility (and hence entrapment) of the hydrophobic drug. This effect has been demonstrated previously, where an increase in the PEG component led to reduced drugs EE (Moribe et al., 1999a, 1999b), and EEs of up to 86% achieved with greater carrier hydrophobicity (Elsaid et al., 2012; Zhou et al., 2010; Zhou et al., 2013). Micelles of LACPEG/DSPE-PEG had a higher EE than LACPEG micelles (80.3% compared to 45.6%, $p<0.05$); in line with other studies using lipid-based micelles to entrap hydrophobic drugs, reporting EEs greater than 89% (Chitkara, 2012). Increasing the content of the hydrophobic moiety (and reducing the hydrophilic component) of micelles (e.g. PEG-PE/vitamin E micelles) has led to increased EE of hydrophobic drugs (Sarisozen et al., 2012). Additionally, the high EE of the LACPEG/DSPE-PEG micelles may result from molecular interactions between the amino group in the chitosan of LACPEG and the phosphate group in the DSPE-PEG portion of the micelles, causing both polymers to form micelles with a more hydrophobic core than LACPEG micelles, improving hydrophobic drug entrapment. A similar molecular interaction has been reported between the amino groups of nystatin and the phosphate groups of DSPE-PEG micelles (Moribe et al., 1999a). The DSPE-PEG component of the LACPEG/DSPE-PEG micelles could also be playing a greater role in the high EE of the mixed micelles as there was no statistically significant difference in the EEs of both micelles (DSPE-PEG was 80.9 % and LACPEG/DSPE-PEG was 80.3%).

The viability of A549 and PC-9 cells was assessed following exposure to drug solution, empty and drug-loaded micelles for 72 h (Fig. 5). The cytotoxic effect of the empty micelles was in the order: LACPEG > DSPE-PEG > LACPEG/DSPE-PEG, for both cell lines. This may be due to several

factors, namely micelle size, charge, PEG content and the number of polymer chains. Studies have shown that smaller nanocarriers are associated with greater induction of oxidative stress and hence toxicity (Jiang et al., 2009; Simon-Deckers et al., 2009). However, LACPEG micelles were larger than those of both DSPE-PEG and LACPEG/DSPE-PEG (Fig. 2) and showed greater cell death, indicating size is not the only determinant of cytotoxicity.

Micellar charge may also influence toxicity (Table 1). A higher positive charge, as for LACPEG micelles, because of the chitosan component, has been associated with toxicity (Kean et al., 2005). Mixed micelles of LACPEG/DSPE-PEG had a lower positive charge compared to LACPEG micelles (Table 1), due to the addition of the negatively charged DSPE-PEG, and increasing the PEG component, which masks the charge (Malhotra et al., 2013; Sezgin et al., 2006) and reduces cytotoxicity (Malhotra et al., 2013). This was seen with the LACPEG/DSPE-PEG micelles, which were least toxic in both cell lines. Perhaps the cancer cell death observed with the LACPEG micelles is not an indicator of toxicity but instead an observation of the carrier's apoptotic potential towards cancer cell lines. For instance, its lipoic acid component, has been shown to inhibit cell proliferation and growth, as well as induce the selective apoptosis of a number of cancer cell lines (through the downregulation of the BCL-2 protein), including lung cancer cells (Choi et al., 2009; Dozio et al., 2010; Michikoshi et al., 2013; Moungjaroen et al., 2006; Na et al., 2009; Wenzel et al., 2005). Furthermore, previous studies have also shown that chitosan inhibits cell proliferation and metastases, as well as induces apoptosis (Hasegawa et al., 2001; Kim et al., 2013). The cationic nature of LACPEG could also enhance the cellular uptake of the carrier (Peetla et al., 2014), which could, in turn, increase these effects.

The concentration of micelles in the drug-loaded micelles (Fig. 5 C and D) equalled that used in the empty micelles (Fig. 5 A and B). Drug-loaded LACPEG micelles had a 1.7-fold lower IC50 value than the drug solution in A549 cells, thereby increasing the sensitivity of this drug-refractory cell line. This was not the case with drug-loaded DSPE-PEG and LACPEG/DSPE-PEG micelles. This suggests a greater effect imparted from the LACPEG micelles, corresponding with empty LACPEG micelles have

greater apoptotic effect than DSPE-PEG and LACPEG/DSPE-PEG micelles, thereby augmenting the effect of the drug.

The order of cancer cell death of drug-loaded micelles in A549 cells (LACPEG > LACPEG/DSPE-PEG> DSPE-PEG) differed to PC-9 cells (DSPE-PEG > LACPEG > LACPEG/DSPE-PEG). This may relate to cell specific variations in micelle uptake, dissociation rate (and hence the rate of drug release), as well as micelle stability with respect to their endosomal escape and subcellular distribution. For instance, polyhistidine (PHIS)-PEG/DSPE-PEG micelles were unstable at pH <6, dissociating in the tumor environment, resulting in greater release of paclitaxel (and thus cytotoxicity) compared to DSPE-PEG micelles (Wu et al., 2013). The cellular uptake and endosomal escape in the tumor microenvironment for DSPE-PEG micelles is dependent on the degree of saturation of the alkyl chain (Bast, 2014).

These data, obtained using the MTS assay, were confirmed using the Live/Dead assay (Fig. 6), with greater cell death seen with A549 and PC-9 cells exposed to drug solution and drug-loaded micelles compared to their empty counterparts.

The mixed LACPEG/DSPE-PEG micelles were taken forward for further analysis, *in vivo*, using the CT26-tumor bearing BALB/c and LLC-tumor bearing C57/BL6 mice models, for multiple reasons. They demonstrated a unique condensation effect with drug loading in addition to high entrapment efficiency, prolonged physical stability and an enhanced thermal stability. Further, the LACPEG/DSPE-PEG mixed micelles demonstrated a better safety profile relative to the single micelles. DSPE-PEG micelles were used in these *in vivo* studies as a comparative micelle system, given that it had a higher EE and better safety profile compared to LACPEG micelles.

For CT26-tumor bearing BALB/c mice (Fig. 7 A-C), DiI-incorporated LACPEG/DSPE-PEG and DSPE-PEG micelles showed a prolonged circulation half-life and higher tumor accumulation than PLGA microparticles (negative control). The lower tumor accumulation observed with the PLGA microparticles may be attributed to their large size and consequent rapid clearance from the blood, with liver and spleen accumulation (Lecaroz et al., 2007). These results were confirmed with *ex vivo*

studies carried out after 24 h. The CT26-tumor bearing BALB/c mouse is a highly vascularised cancer model (Seguin et al., 2013), with tumor accumulation influenced namely by circulation half-lives, and to a lesser extent nanocarrier size. Nanocarriers of less than 200 nm with components reported to improve circulation half-lives, such as those incorporating polyethylene glycol (PEG), can exploit the EPR effect, passively entering and accumulating in tumors (Maruyama, 2011). In this study, DSPE-PEG and LACPEG/DSPE-PEG micelles, showed no difference in tumor accumulation (Fig. 7 C, where the fluorescence intensities quantified were divided by the weight of each organ and normalised to the liver, to account for variations in tissue weight and DiI dose injected, respectively) even though they differed in size (30 nm and 100 nm, respectively) and PEG content (2 and 7 kDa, respectively). Micelles with PEG molecular weights $\geq$ 2 kDa have prolonged circulation half-lives and increased deposition at tumor sites (Duan and Li, 2013; Gao et al., 2013; Lipka et al., 2010).

Similar results were seen with the LLC-tumor bearing C57/BL6 mouse model (Fig. 7 D and E). This is a low vascularised model, with tumor accumulation influenced to a greater extent by nanocarrier size (Weissig et al., 1998). Previous studies have shown that tumor accumulation is inversely related to nanocarrier size. For instance, 20 nm DSPE-PEG micelles showed greater accumulation in Lewis Lung tumor *in vivo* than 100 nm liposomes (Weissig et al., 1998). Tumor accumulation was observed for both LACPEG/DSPE-PEG and DSPE-PEG micelles over 24 h despite differences in sizes (100 and 35 nm, respectively). Thus, these micelles allow for tumor accumulation in multiple tumor models.

Flow cytometric analysis of tumor cell suspensions *ex vivo* showed comparable mean fluorescence intensities for both DSPE-PEG and LACPEG/DSPE-PEG micelles treatments (p=0.05) (Fig. 8). Both were significantly higher (10-12x) than PBS treatment (p<0.05). The fact that a smaller amount of dye was injected into the mice in case of LACPEG/DSPE-PEG (63% DiI loading) than DSPE-PEG (100% DiI loading), due to differences in initial dye loading, indirectly suggests that LACPEG/DSPE-PEG is able to internalise more efficiently into tumor cells than DSPE-PEG. Future studies can be carried out while fixing the DiI dose injected per mouse so that more quantitative *in vivo* tumor uptake data can be generated. The greater efficiency in tumor internalisation for LACPEG/DSPE-PEG micelles compared to DSPE-PEG micelles may be attributed to differences in either delivery to the tumor, accumulation within the endothelium or extravascular component of the tumors, or cellular uptake.

For instance, destabilization of DSPE-PEG micelles has been shown, post injection, on dilution in the blood and following interaction with plasma proteins, resulting in premature release of encapsulated agents prior to the micelles reaching their target site (Castelletto et al., 2007; Kastantin et al., 2010). Mixed micelles, on the other hand, have been shown to possess greater *in vivo* stability, resulting from the shielding of the hydrophobic components of the carrier, from the plasma proteins, by their greater PEG content (Li et al., 2011). In this study, LACPEG/DSPE-PEG micelles showed greater stability than DSPE-PEG micelles (showing no signs of aggregation on storage) and a greater interaction with the hydrophobic drug (as evidenced by the reduction in size post entrapment with the mixed micelles). Therefore, due to their enhanced stability, mixed micelles could show greater tumor accumulation than standard micelles. Although the LACPEG/DSPE-PEG and DSPE-PEG micelles showed no significant difference in tumor accumulation, as discussed above (Fig. 7C), the data collected does not distinguish between the endothelium of the tumor and the extravascular component. It is possible that the positively-charged LACPEG/DSPE-PEG micelles have accumulated within the endothelium and hence shown greater cellular internalisation than the negatively-charged DSPE-PEG micelles, given that studies have shown that cationic carriers preferentially target and accumulate within the angiogenic endothelium of tumors compared to anionic carriers, which distribute into the extravascular compartment of tumors due to their extravasation (Krasnici et al., 2003). Cellular uptake is also governed by the surface characteristics of the carrier (i.e. its hydrophobicity and charge) and its size. Hydrophobic carriers interact with the lipid bilayer of cell membranes to a greater extent than hydrophilic carriers, cationic carriers show greater interaction with the anionic cell membrane compared to anionic carriers and are more like to escape from endosomes after internalization due to the 'proton-sponge' effect, and smaller nanoparticles show more rapid cellular uptake than larger particles (Kou et al., 2013). In the case of LACPEG/DSPE-PEG micelles, their greater cellular internalisation when compared to DSPE-PEG, may be associated with the hydrophobicity (additional lipoic acid component) and charge (positive compared to the negatively-charged DSPE-PEG), rather than size, as the micelles are larger than for those of DSPE-PEG (100 nm compared to 30 nm for the empty micelles and 49.8 nm compared to 26.7 nm for the drug-loaded micelles). The smaller size of DSPE-PEG micelles could be contributing to a fast rate of exocytosis from the cell, an effect shown with nanoparticles < 50 nm, including mixed micelles of

TPGS/Pluronic (Cao et al., 2016; Jiang et al., 2010; Oh et al., 2004; Serda et al., 2010). It should be noted that although the hydrophilic components (chitosan and PEG) are greater in the mixed micelles, and studies have shown these components suppress the carriers' hydrophobic interaction with the cell membrane and reduce uptake (Kou et al., 2013), they can help prolong the circulation time of nanocarriers in the blood and allow them to reach the target site, as was observed with the micelles in this study.

Despite the effectiveness of chemotherapeutic agents for treatment of cancer, they often possess a number of limitations, including poor water solubility, bioavailability and tumor accumulation. The objectives of this study were to synthesize a novel amphiphilic polymer; LACPEG and use this polymer alone, or mixed with DSPE-PEG, to prepare drug-loaded micelles. These objectives were met with production of drug-loaded micelles having mean sizes less than 130 nm and entrapment efficiencies up to 81%. LACPEG inclusion improved the physical stability of the drug-loaded micelles. Empty LACPEG and DSPE-PEG micelles showed greater toxicity than LACPEG/DSPE-PEG micelles. The apoptotic potential of LACPEG micelles should be investigated in future studies. DSPE-PEG and LACPEG/DSPE-PEG micelles were taken forward for animal studies and showed prolonged whole body circulation and significant tumor accumulation in CT26-tumor bearing BALB/c and LLC-tumor bearing C57/BL6 mice. Although LACPEG/DSPE-PEG micelles showed similar drug loading to DSPE-PEG micelles, LACPEG/DSPE-PEG micelles are particularly attractive as they had greater size stability over 30 days, lower *in vitro* toxicity and is able to internalise more efficiently into tumor cells. These findings suggest that LACPEG and LACPEG/DSPE-PEG micelles may be considered as future platforms for delivery of poorly water soluble anticancer drugs.

Acknowledgements: We thank Dr Paul Stapleton and Mr David McCarthy and for their assistance in the Live/Dead assay and TEM.

Abbreviations used: LACPEG, lipoic acid-chitosan-poly(ethylene glycol); DSPE-PEG, distearoylphosphatidylethanolamine-poly(ethylene glycol).

References

Adams, M.L., Kwon, G.S., 2003. Relative aggregation state and hemolytic activity of amphotericin B encapsulated by poly(ethylene oxide)-block-poly(N-hexyl-L-aspartamide)-acyl conjugate micelles: effects of acyl chain length. Journal of controlled release : official journal of the Controlled Release Society 87, 23-32.
Alexis, F., Pridgen, E., Molnar, L.K., Farokhzad, O.C., 2008. Factors affecting the clearance and biodistribution of polymeric nanoparticles. Molecular pharmaceutics 5, 505-515.
Aranaz, I.H., R.; Heras, A, 2010. Chitosan Amphiphilic Derivatives. Chemistry and Applications. Current Organic Chemistry 14, 308-330
Ashok, B., Arleth, L., Hjelm, R.P., Rubinstein, I., Onyuksel, H., 2004. In vitro characterization of PEGylated phospholipid micelles for improved drug solubilization: effects of PEG chain length and PC incorporation. Journal of pharmaceutical sciences 93, 2476-2487.
Attia, A.B., Yang, C., Tan, J.P., Gao, S., Williams, D.F., Hedrick, J.L., Yang, Y.Y., 2013. The effect of kinetic stability on biodistribution and anti-tumor efficacy of drug-loaded biodegradable polymeric micelles. Biomaterials 34, 3132-3140.
Bast, R.C., M. Markman, and E. Hawk, 2014. Delivery systems: extravasation, targeting and internalization Cancer gene therapy by viral and non-viral vectors. Wiley Blackwell, UK.
Burris, H.A., Infante, J.R., Anthony Greco, F., Thompson, D.S., Barton, J.H., Bendell, J.C., Nambu, Y., Watanabe, N., Jones, S.F., 2016. A phase I dose escalation study of NK012, an SN-38 incorporating macromolecular polymeric micelle. Cancer chemotherapy and pharmacology 77, 1079-1086.
Butt, A.M., Amin, M.C.I.M., Katas, H., Sarisuta, N., Witoonsaridsilp, W., Benjakul, R., 2012. In Vitro Characterization of Pluronic F127 and D--Tocopheryl Polyethylene Glycol 1000 Succinate Mixed Micelles as Nanocarriers for Targeted Anticancer-Drug Delivery. Journal of Nanomaterials 2012, 11.
Cao, X., Zhou, X., Wang, Y., Gong, T., Zhang, Z.-R., Liu, R., Fu, Y., 2016. Diblock- and triblock-copolymer based mixed micelles with high tumor penetration in vitro and in vivo. Journal of Materials Chemistry B 4, 3216-3224.
Castelletto, V., Krysmann, M., Kelarakis, A., Jauregi, P., 2007. Complex formation of bovine serum albumin with a poly(ethylene glycol) lipid conjugate. Biomacromolecules 8, 2244-2249.
Chen, L., Sha, X., Jiang, X., Chen, Y., Ren, Q., Fang, X., 2013. Pluronic P105/F127 mixed micelles for the delivery of docetaxel against Taxol-resistant non-small cell lung cancer: optimization and in vitro, in vivo evaluation. International journal of nanomedicine 8, 73-84.
Chitkara, D.S., S.; Kumar, V.; Danquah, M.; Behrman, S. W.; Kumar, N.; Mahato, R. I, 2012. Micellar delivery of cyclopamine and gefitinib for treating pancreatic cancer. Molecular pharmaceutics 9, 2350-2357.
Choi, S.Y., Yu, J.H., Kim, H., 2009. Mechanism of alpha-lipoic acid-induced apoptosis of lung cancer cells. Annals of the New York Academy of Sciences 1171, 149-155.
Deol, P., Khuller, G.K., 1997. Lung specific stealth liposomes: stability, biodistribution and toxicity of liposomal antitubercular drugs in mice. Biochimica et biophysica acta 1334, 161-172.
Diao, Y.Y., Li, H.Y., Fu, Y.H., Han, M., Hu, Y.L., Jiang, H.L., Tsutsumi, Y., Wei, Q.C., Chen, D.W., Gao, J.Q., 2011. Doxorubicin-loaded PEG-PCL copolymer micelles enhance cytotoxicity and intracellular accumulation of doxorubicin in adriamycin-resistant tumor cells. International journal of nanomedicine 6, 1955-1962.
Dozio, E., Ruscica, M., Passafaro, L., Dogliotti, G., Steffani, L., Pagani, A., Demartini, G., Esposti, D., Fraschini, F., Magni, P., 2010. The natural antioxidant alpha-lipoic acid induces p27Kip1-dependent cell cycle arrest and apoptosis in MCF-7 human breast cancer cells. European Journal of Pharmacology 641, 29-34.
Duan, B., Dong, C., Yuan, X., Yao, K., 2004. Electrospinning of chitosan solutions in acetic acid with poly(ethylene oxide). Journal of biomaterials science. Polymer edition 15, 797-811.
Duan, X., Li, Y., 2013. Physicochemical characteristics of nanoparticles affect circulation, biodistribution, cellular internalization, and trafficking. Small (Weinheim an der Bergstrasse, Germany) 9, 1521-1532.
Ebrahim Attia, A.B., Ong, Z.Y., Hedrick, J.L., Lee, P.P., Ee, P.L.R., Hammond, P.T., Yang, Y.-Y., 2011. Mixed micelles self-assembled from block copolymers for drug delivery. Current Opinion in Colloid & Interface Science 16, 182-194.
Elsaid, N., Jackson, T.L., Gunic, M., Somavarapu, S., 2012. Positively charged amphiphilic chitosan derivative for the transscleral delivery of rapamycin. Investigative ophthalmology & visual science 53, 8105-8111.
Farhat, F.S., Houhou, W., 2013. Targeted therapies in non-small cell lung carcinoma: what have we achieved so far? Therapeutic Advances in Medical Oncology 5, 249-270.

Gao, H., Liu, J., Yang, C., Cheng, T., Chu, L., Xu, H., Meng, A., Fan, S., Shi, L., Liu, J., 2013. The impact of PEGylation patterns on the in vivo biodistribution of mixed shell micelles. International journal of nanomedicine 8, 4229-4246.
Gao, Y., Li, L.B., Zhai, G., 2008. Preparation and characterization of Pluronic/TPGS mixed micelles for solubilization of camptothecin. Colloids and Surfaces B: Biointerfaces 64, 194-199.
Guan, S.-S., Chang, J., Cheng, C.-C., Luo, T.-Y., Ho, A.-S., Wang, C.-C., Wu, C.-T., Liu, S.-H., 2014. Afatinib and its encapsulated polymeric micelles inhibits HER2-overexpressed colorectal tumor cell growth in vitro and in vivo. Oncotarget 5, 4868-4880.
Haag, R., 2004. Supramolecular drug-delivery systems based on polymeric core-shell architectures. Angewandte Chemie (International ed. in English) 43, 278-282.
Hasegawa, M., Yagi, K., Iwakawa, S., Hirai, M., 2001. Chitosan induces apoptosis via caspase-3 activation in bladder tumor cells. Japanese journal of cancer research : Gann 92, 459-466.
Hashizaki, K., Taguchi, H., Itoh, C., Sakai, H., Abe, M., Saito, Y., Ogawa, N., 2003. Effects of poly(ethylene glycol) (PEG) chain length of PEG-lipid on the permeability of liposomal bilayer membranes. Chemical & pharmaceutical bulletin 51, 815-820.
Huang, Y., Yu, H., Guo, L., Huang, Q., 2010. Structure and Self-Assembly Properties of a New Chitosan-Based Amphiphile. The Journal of Physical Chemistry B 114, 7719-7726.
Jiang, J., Oberdörster, G., Biswas, P., 2009. Characterization of size, surface charge, and agglomeration state of nanoparticle dispersions for toxicological studies. J Nanopart Res 11, 77-89.
Jiang, X., Rocker, C., Hafner, M., Brandholt, S., Dorlich, R.M., Nienhaus, G.U., 2010. Endo- and exocytosis of zwitterionic quantum dot nanoparticles by live HeLa cells. ACS nano 4, 6787-6797.
Johnsson, M., Hansson, P., Edwards, K., 2001. Spherical Micelles and Other Self-Assembled Structures in Dilute Aqueous Mixtures of Poly(Ethylene Glycol) Lipids. The Journal of Physical Chemistry B 105, 8420-8430.
Kahook, M.Y., Liu, L., Ruzycki, P., Mandava, N., Carpenter, J.F., Petrash, J.M., Ammar, D.A., 2010. High-molecular-weight aggregates in repackaged bevacizumab. Retina (Philadelphia, Pa.) 30, 887-892.
Kastantin, M., Missirlis, D., Black, M., Ananthanarayanan, B., Peters, D., Tirrell, M., 2010. Thermodynamic and kinetic stability of DSPE-PEG(2000) micelles in the presence of bovine serum albumin. The journal of physical chemistry. B 114, 12632-12640.
Kean, T., Roth, S., Thanou, M., 2005. Trimethylated chitosans as non-viral gene delivery vectors: cytotoxicity and transfection efficiency. Journal of controlled release : official journal of the Controlled Release Society 103, 643-653.
Kim, M.-O., Moon, D.-O., Kang, C.-H., Choi, Y.H., Lee, J.-D., Kim, G.-Y., 2013. Water-soluble chitosan sensitizes apoptosis in human leukemia cells via the downregulation of BCL-2 and dephosphorylation of AKT. J Food Biochem 37, 270-277.
Kim, S., Shi, Y., Kim, J.Y., Park, K., Cheng, J.X., 2010. Overcoming the barriers in micellar drug delivery: loading efficiency, in vivo stability, and micelle-cell interaction. Expert Opin Drug Deliv 7, 49-62.
Kim, S.C., Kim, D.W., Shim, Y.H., Bang, J.S., Oh, H.S., Wan Kim, S., Seo, M.H., 2001. In vivo evaluation of polymeric micellar paclitaxel formulation: toxicity and efficacy. Journal of controlled release : official journal of the Controlled Release Society 72, 191-202.
Koizumi, F., Kitagawa, M., Negishi, T., Onda, T., Matsumoto, S., Hamaguchi, T., Matsumura, Y., 2006. Novel SN-38-incorporating polymeric micelles, NK012, eradicate vascular endothelial growth factor-secreting bulky tumors. Cancer research 66, 10048-10056.
Kou, L., Sun, J., Zhai, Y., He, Z., 2013. The endocytosis and intracellular fate of nanomedicines: Implication for rational design. Asian Journal of Pharmaceutical Sciences 8, 1-10.
Krasnici, S., Werner, A., Eichhorn, M.E., Schmitt-Sody, M., Pahernik, S.A., Sauer, B., Schulze, B., Teifel, M., Michaelis, U., Naujoks, K., Dellian, M., 2003. Effect of the surface charge of liposomes on their uptake by angiogenic tumor vessels. International journal of cancer 105, 561-567.
Kulthe, S., Inamdar, N., Godhani, C., Choudhari, Y., Shirolikar, S., Borde, L., Thanki, K., Agrawal, M., Agrawal, S.K., Jain, S., Mourya, V., 2014. Mixed Micellar Nanocarriers for Controlled and Targeted Delivery of Paclitaxel. Journal of Nanopharmaceutics and Drug Delivery 2, 69-79.
Kumirska, J., Czerwicka, M., Kaczynski, Z., Bychowska, A., Brzozowski, K., Thoming, J., Stepnowski, P., 2010. Application of spectroscopic methods for structural analysis of chitin and chitosan. Marine drugs 8, 1567-1636.
Lecaroz, M.C., Blanco-Prieto, M.J., Campanero, M.A., Salman, H., Gamazo, C., 2007. Poly(D,L-lactide-coglycolide) particles containing gentamicin: pharmacokinetics and pharmacodynamics in Brucella melitensis-infected mice. Antimicrobial agents and chemotherapy 51, 1185-1190.

Lee, J., Cho, E.C., Cho, K., 2004. Incorporation and release behavior of hydrophobic drug in functionalized poly(D,L-lactide)-block-poly(ethylene oxide) micelles. Journal of controlled release : official journal of the Controlled Release Society 94, 323-335.
Lee, Y.S., Johnson, P.J., Robbins, P.T., Bridson, R.H., 2013. Production of nanoparticles-in-microparticles by a double emulsion method: A comprehensive study. European journal of pharmaceutics and biopharmaceutics : official journal of Arbeitsgemeinschaft fur Pharmazeutische Verfahrenstechnik e.V 83, 168-173.
Li, X., Zhang, Y., Fan, Y., Zhou, Y., Wang, X., Fan, C., Liu, Y., Zhang, Q., 2011. Preparation and evaluation of novel mixed micelles as nanocarriers for intravenous delivery of propofol. Nanoscale Research Letters 6, 1-9.
Lin, H.R., Chang, P.C., 2013. Novel pluronic-chitosan micelle as an ocular delivery system. Journal of biomedical materials research. Part B, Applied biomaterials 101, 689-699.
Lipka, J., Semmler-Behnke, M., Sperling, R.A., Wenk, A., Takenaka, S., Schleh, C., Kissel, T., Parak, W.J., Kreyling, W.G., 2010. Biodistribution of PEG-modified gold nanoparticles following intratracheal instillation and intravenous injection. Biomaterials 31, 6574-6581.
Maeda, H., 2001. The enhanced permeability and retention (EPR) effect in tumor vasculature: the key role of tumor-selective macromolecular drug targeting. Advances in enzyme regulation 41, 189-207.
Maeda, H., Nakamura, H., Fang, J., 2013. The EPR effect for macromolecular drug delivery to solid tumors: Improvement of tumor uptake, lowering of systemic toxicity, and distinct tumor imaging in vivo. Advanced drug delivery reviews 65, 71-79.
Maeda, H., Wu, J., Sawa, T., Matsumura, Y., Hori, K., 2000. Tumor vascular permeability and the EPR effect in macromolecular therapeutics: a review. Journal of controlled release : official journal of the Controlled Release Society 65, 271-284.
Malhotra, M., Tomaro-Duchesneau, C., Saha, S., Kahouli, I., Prakash, S., 2013. Development and characterization of chitosan-PEG-TAT nanoparticles for the intracellular delivery of siRNA. International journal of nanomedicine 8, 2041-2052.
Maruyama, K., 2011. Intracellular targeting delivery of liposomal drugs to solid tumors based on EPR effects. Advanced drug delivery reviews 63, 161-169.
Maruyama, K., Yuda, T., Okamoto, A., Kojima, S., Suginaka, A., Iwatsuru, M., 1992. Prolonged circulation time in vivo of large unilamellar liposomes composed of distearoyl phosphatidylcholine and cholesterol containing amphipathic poly(ethylene glycol). Biochimica et biophysica acta 1128, 44-49.
Matsumura, Y., Maeda, H., 1986. A new concept for macromolecular therapeutics in cancer chemotherapy: mechanism of tumoritropic accumulation of proteins and the antitumor agent smancs. Cancer research 46, 6387-6392.
Michikoshi, H., Nakamura, T., Sakai, K., Suzuki, Y., Adachi, E., Matsugo, S., Matsumoto, K., 2013. alpha-Lipoic acid-induced inhibition of proliferation and met phosphorylation in human non-small cell lung cancer cells. Cancer letters 335, 472-478.
Moribe, K., Maruyama, K., Iwatsuru, M., 1999a. Molecular localization and state of amphotericin B in PEG liposomes. International journal of pharmaceutics 193, 97-106.
Moribe, K., Maruyama, K., Iwatsuru, M., 1999b. Encapsulation characteristics of nystatin in liposomes: effects of cholesterol and polyethylene glycol derivatives. International journal of pharmaceutics 188, 193-202.
Moungjaroen, J., Nimmannit, U., Callery, P.S., Wang, L., Azad, N., Lipipun, V., Chanvorachote, P., Rojanasakul, Y., 2006. Reactive oxygen species mediate caspase activation and apoptosis induced by lipoic acid in human lung epithelial cancer cells through Bcl-2 down-regulation. The Journal of pharmacology and experimental therapeutics 319, 1062-1069.
Na, M.H., Seo, E.Y., Kim, W.K., 2009. Effects of alpha-lipoic acid on cell proliferation and apoptosis in MDA-MB-231 human breast cells. Nutrition research and practice 3, 265-271.
Nasr, M., Mansour, S., Mortada, N.D., El Shamy, A.A., 2008. Lipospheres as carriers for topical delivery of aceclofenac: preparation, characterization and in vivo evaluation. AAPS PharmSciTech 9, 154-162.
Oh, K.T., Bronich, T.K., Kabanov, A.V., 2004. Micellar formulations for drug delivery based on mixtures of hydrophobic and hydrophilic Pluronic block copolymers. Journal of controlled release : official journal of the Controlled Release Society 94, 411-422.
Peetla, C., Jin, S., Weimer, J., Elegbede, A., Labhasetwar, V., 2014. Biomechanics and thermodynamics of nanoparticle interactions with plasma and endosomal membrane lipids in cellular uptake and endosomal escape. Langmuir : the ACS journal of surfaces and colloids 30, 7522-7532.
Pepic, I., Lovric, J., Hafner, A., Filipovic-Grcic, J., 2014. Powder form and stability of Pluronic mixed micelle dispersions for drug delivery applications. Drug development and industrial pharmacy 40, 944-951.

Pillai, G., 2014. Nanomedicines for Cancer Therapy: An Update of FDA Approved and Those under Various Stages of Development. SOJ Pharm Pharm Sci 1, 1-13.
Remsberg, C.M., Zhao, Y., Takemoto, J.K., Bertram, R.M., Davies, N.M., Forrest, M.L., 2012. Pharmacokinetic Evaluation of a DSPE-PEG2000 Micellar Formulation of Ridaforolimus in Rat. Pharmaceutics 5, 81-93.
Reuter, S., Gupta, S.C., Chaturvedi, M.M., Aggarwal, B.B., 2010. Oxidative stress, inflammation, and cancer: How are they linked? Free radical biology & medicine 49, 1603-1616.
Ribeiro, A., Sosnik A Fau - Chiappetta, D.A., Chiappetta Da Fau - Veiga, F., Veiga F Fau - Concheiro, A., Concheiro A Fau - Alvarez-Lorenzo, C., Alvarez-Lorenzo, C., 2012. Single and mixed poloxamine micelles as nanocarriers for solubilization and sustained release of ethoxzolamide for topical glaucoma therapy.
Sarisozen, C., Vural, I., Levchenko, T., Hincal, A.A., Torchilin, V.P., 2012. PEG-PE-based micelles co-loaded with paclitaxel and cyclosporine A or loaded with paclitaxel and targeted by anticancer antibody overcome drug resistance in cancer cells. Drug delivery 19, 169-176.
Seguin, J., Doan, B.-T., Latorre Ossa, H., Jug, #xe9, , L., Gennisson, J.-L., Tanter, M., #xeb, Scherman, D., Chabot, G.G., Mignet, N., 2013. Evaluation of Nonradiative Clinical Imaging Techniques for the Longitudinal Assessment of Tumour Growth in Murine CT26 Colon Carcinoma. International Journal of Molecular Imaging 2013, 13.
Serda, R.E., Mack, A., van de Ven, A.L., Ferrati, S., Dunner, K., Jr., Godin, B., Chiappini, C., Landry, M., Brousseau, L., Liu, X., Bean, A.J., Ferrari, M., 2010. Logic-embedded vectors for intracellular partitioning, endosomal escape, and exocytosis of nanoparticles. Small (Weinheim an der Bergstrasse, Germany) 6, 2691-2700.
Sezgin, Z., Yuksel, N., Baykara, T., 2006. Preparation and characterization of polymeric micelles for solubilization of poorly soluble anticancer drugs. European journal of pharmaceutics and biopharmaceutics : official journal of Arbeitsgemeinschaft fur Pharmazeutische Verfahrenstechnik e.V 64, 261-268.
Simon-Deckers, A., Loo, S., Mayne-L'hermite, M., Herlin-Boime, N., Menguy, N., Reynaud, C., Gouget, B., Carrière, M., 2009. Size-, Composition- and Shape-Dependent Toxicological Impact of Metal Oxide Nanoparticles and Carbon Nanotubes toward Bacteria. Environmental Science & Technology 43, 8423-8429.
Slager, T.L., Prozonic, F.M., 2005. Simple methods for calibrating IR in TGA/IR analyses. Thermochimica Acta 426, 93-99.
Sogias, I.A., Williams, A.C., Khutoryanskiy, V.V., 2008. Why is chitosan mucoadhesive? Biomacromolecules 9, 1837-1842.
Tian, Y., Mao, S., 2012. Amphiphilic polymeric micelles as the nanocarrier for peroral delivery of poorly soluble anticancer drugs. Expert Opin Drug Deliv 9, 687-700.
Torchilin, V.P., 2001. Structure and design of polymeric surfactant-based drug delivery systems. Journal of controlled release : official journal of the Controlled Release Society 73, 137-172.
Torchilin, V.P., 2007. Micellar nanocarriers: pharmaceutical perspectives. Pharmaceutical research 24, 1-16.
Tursilli, R., Casolari, A., Iannuccelli, V., Scalia, S., 2006. Enhancement of melatonin photostability by encapsulation in lipospheres. Journal of pharmaceutical and biomedical analysis 40, 910-914.
Varshosaz, J., Taymouri, S., Hassanzadeh, F., Haghjooy Javanmard, S., Rostami, M., 2015. Folated Synperonic-Cholesteryl Hemisuccinate Polymeric Micelles for the Targeted Delivery of Docetaxel in Melanoma. BioMed Research International 2015, 17.
Wang, R., Xiao, R., Zeng, Z., Xu, L., Wang, J., 2012. Application of poly(ethylene glycol)-distearoylphosphatidylethanolamine (PEG-DSPE) block copolymers and their derivatives as nanomaterials in drug delivery. International journal of nanomedicine 7, 4185-4198.
Wang, Y., Fan, W., Dai, X., Katragadda, U., McKinley, D., Teng, Q., Tan, C., 2014. Enhanced Tumor Delivery of Gemcitabine via PEG-DSPE/TPGS Mixed Micelles. Molecular pharmaceutics 11, 1140-1150.
Weerakody, R., Fagan, P., Kosaraju, S.L., 2008. Chitosan microspheres for encapsulation of alpha-lipoic acid. International journal of pharmaceutics 357, 213-218.
Weissig, V., Whiteman, K.R., Torchilin, V.P., 1998. Accumulation of protein-loaded long-circulating micelles and liposomes in subcutaneous Lewis lung carcinoma in mice. Pharmaceutical research 15, 1552-1556.
Wenzel, U., Nickel, A., Daniel, H., 2005. alpha-Lipoic acid induces apoptosis in human colon cancer cells by increasing mitochondrial respiration with a concomitant O2-*-generation. Apoptosis : an international journal on programmed cell death 10, 359-368.

Wu, H., Zhu, L., Torchilin, V.P., 2013. pH-sensitive poly(histidine)-PEG/DSPE-PEG co-polymer micelles for cytosolic drug delivery. Biomaterials 34, 1213-1222.
Xu, Y., Wen, Z., Xu, Z., 2009. Chitosan nanoparticles inhibit the growth of human hepatocellular carcinoma xenografts through an antiangiogenic mechanism. Anticancer research 29, 5103-5109.
Xue, C., Hong, S., Li, N., Feng, W., Jia, J., Peng, J., Lin, D., Cao, X., Wang, S., Zhang, W., Zhang, H., Dong, W., Zhang, L., 2015. Randomized, Multicenter Study of Gefitinib Dose-escalation in Advanced Non-small-cell Lung Cancer Patients Achieved Stable Disease after One-month Gefitinib Treatment. Scientific Reports 5, 10648.
Yang, C.T., J.P.K.; Cheng, W.; Attiaa, A.B.E.; Ting, C.T.Y.; Nelson, A.; Hedrick, J.L.; Yang, Y.Y, 2010. Supramolecular nanostructures designed for high cargo loading capacity and kinetic stability. Nanotoday 5, 515-523. .
Yen, M.-T., Yang, J.-H., Mau, J.-L., 2008. Antioxidant properties of chitosan from crab shells. Carbohydrate Polymers 74, 840-844.
Yuan, H., Lu, L.J., Du, Y.Z., Hu, F.Q., 2011. Stearic acid-g-chitosan polymeric micelle for oral drug delivery: in vitro transport and in vivo absorption. Molecular pharmaceutics 8, 225-238.
Zhang, J., Dang, L., Wei, H., 2013. Thermodynamic analysis of lipoic acid crystallized with additives. J Therm Anal Calorim 111, 2063-2068.
Zhao, B.W., X-Q.; Wang, X-Y.; Zhang, H.; Dai, W-B.; Wang, J.; Zhong, Z-L.; Wu,H-N.; Zhang, Q, 2013. Nanotoxicity comparison of four amphiphilic polymeric micelles with similar hydrophilic or hydrophobic structure. . Particle and Fibre Toxicology 10, 47.
Zhao, L., Du, J., Duan, Y., Zang, Y.n., Zhang, H., Yang, C., Cao, F., Zhai, G., 2012. Curcumin loaded mixed micelles composed of Pluronic P123 and F68: Preparation, optimization and in vitro characterization. Colloids and Surfaces B: Biointerfaces 97, 101-108.
Zhao, L., Raval, V., Briggs, N.E.B., Bhardwaj, R.M., McGlone, T., Oswald, I.D.H., Florence, A.J., 2014. From discovery to scale-up: [small alpha]-lipoic acid : nicotinamide co-crystals in a continuous oscillatory baffled crystalliser. CrystEngComm 16, 5769-5780.
Zheng, P., Zhang, X., Fang, J., Shen, W., 2016. Thermodynamic Study of Mixed Surfactants of Polyoxyethylene tert-Octyl Phenyl Ether and Dodecyltrimethylammonium Bromide. Journal of Chemical & Engineering Data 61, 979-986.
Zhou, H., Yu, W., Guo, X., Liu, X., Li, N., Zhang, Y., Ma, X., 2010. Synthesis and Characterization of Amphiphilic Glycidol−Chitosan−Deoxycholic Acid Nanoparticles as a Drug Carrier for Doxorubicin. Biomacromolecules 11, 3480-3486.
Zhou, W., Wang, Y., Jian, J., Song, S., 2013. Self-aggregated nanoparticles based on amphiphilic poly(lactic acid)-grafted-chitosan copolymer for ocular delivery of amphotericin B. International journal of nanomedicine 8, 3715-3728.

Tables

Table 1. Size, PDI and zeta potential of empty and drug-loaded micelles. Results are expressed as mean ± SD (n=3). Abbreviations: H: hydrophobic drug.

Nanocarrier formulation	Size (nm)	PDI	Zeta Potential (mV)
LACPEG	130 ± 1.25	0.20 ± 0.00	+3.95 ± 1.03
H-loaded LACPEG	115 ± 0.78	0.23 ± 0.01	+5.63 ± 0.98
LACPEG/DSPE-PEG	100 ± 0.62	0.35 ± 0.00	+3.17 ± 0.24
H-load ed LACPEG/DSPE-PEG	49.8 ± 0.26	0.57 ± 0.00	+2.73 ± 0.04
DSPE-PEG	30.1 ± 0.39	0.52 ± 0.01	-1.87 ± 0.07
H-loaded DSPE-PEG	26.7 ± 0.31	0.44 ± 0.01	-1.00 ± 0.02

Table 2. Hydrophobic drug loading and entrapment efficiency for micelles of LACPEG, LACPEG/DSPE-PEG and DSPE-PEG. Results are expressed as mean ± SD (n=3).

Micelles	Drug loading (%)	Entrapment efficiency (%)
LACPEG	2.36 ± 0.03	45.6 ± 0.64
LACPEG/DSPE-PEG	3.83 ± 0.39	80.3 ± 8.16
DSPE-PEG	4.03 ± 0.46	80.9 ± 9.16

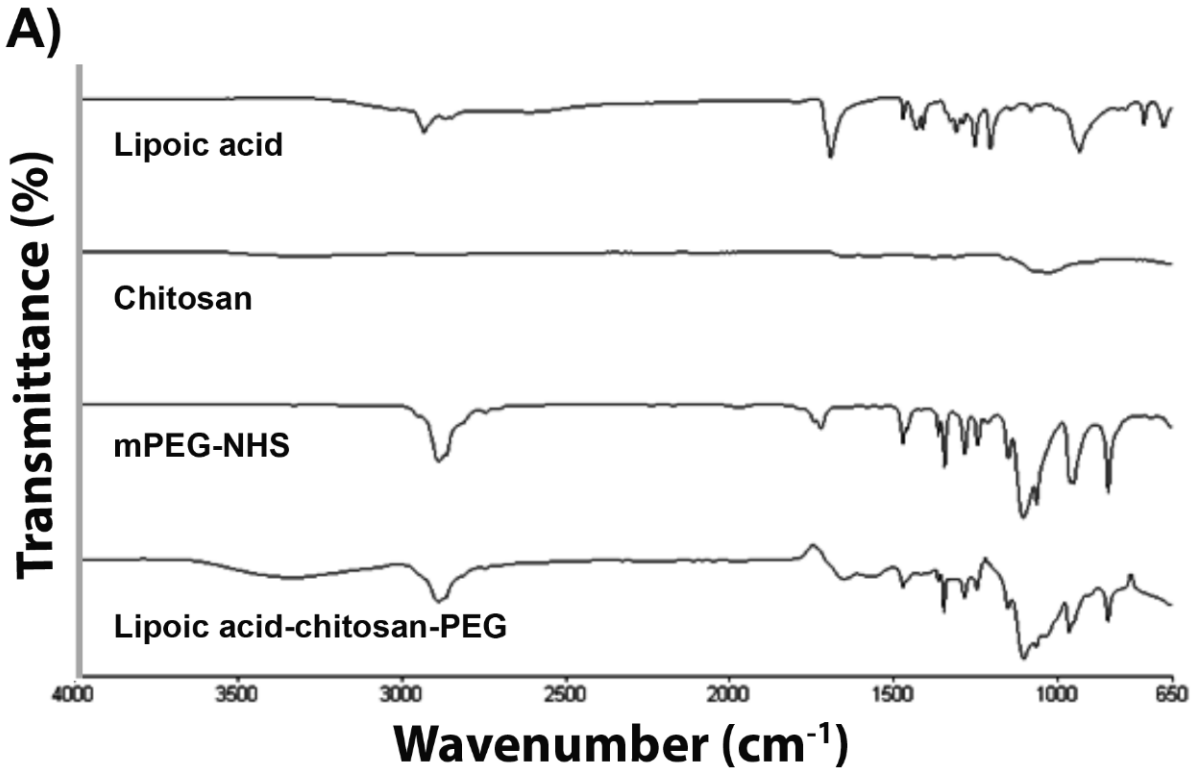

Fig. 1a

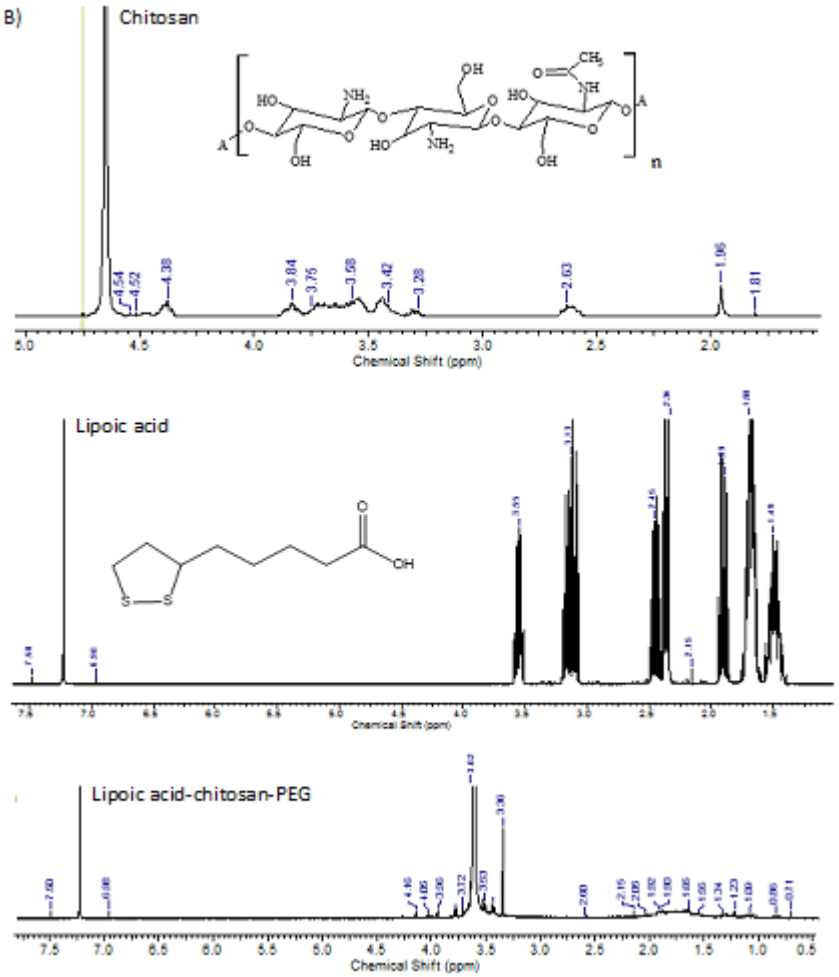

Fig. 1b

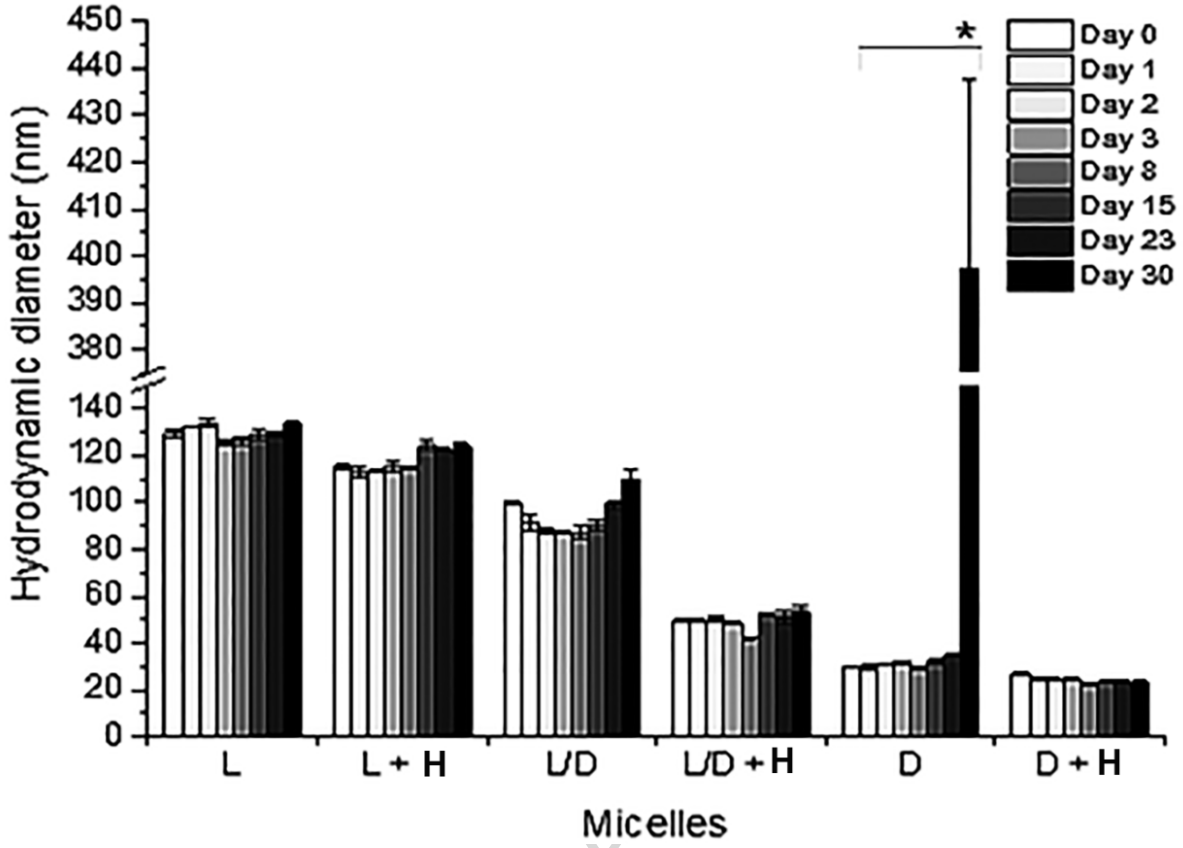

Fig. 2

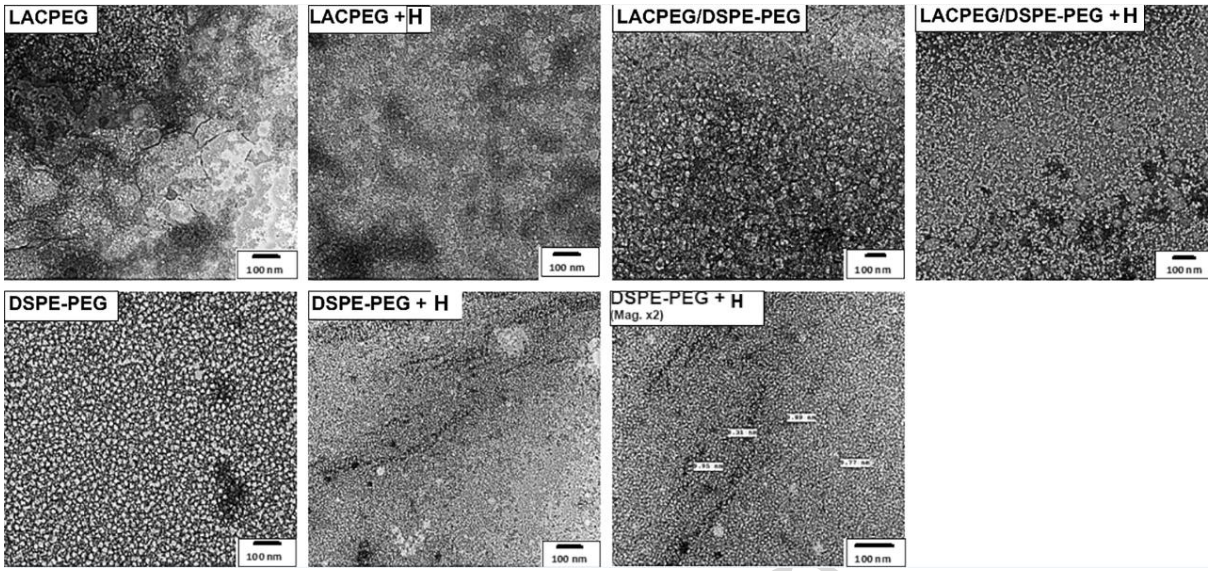

Fig. 3

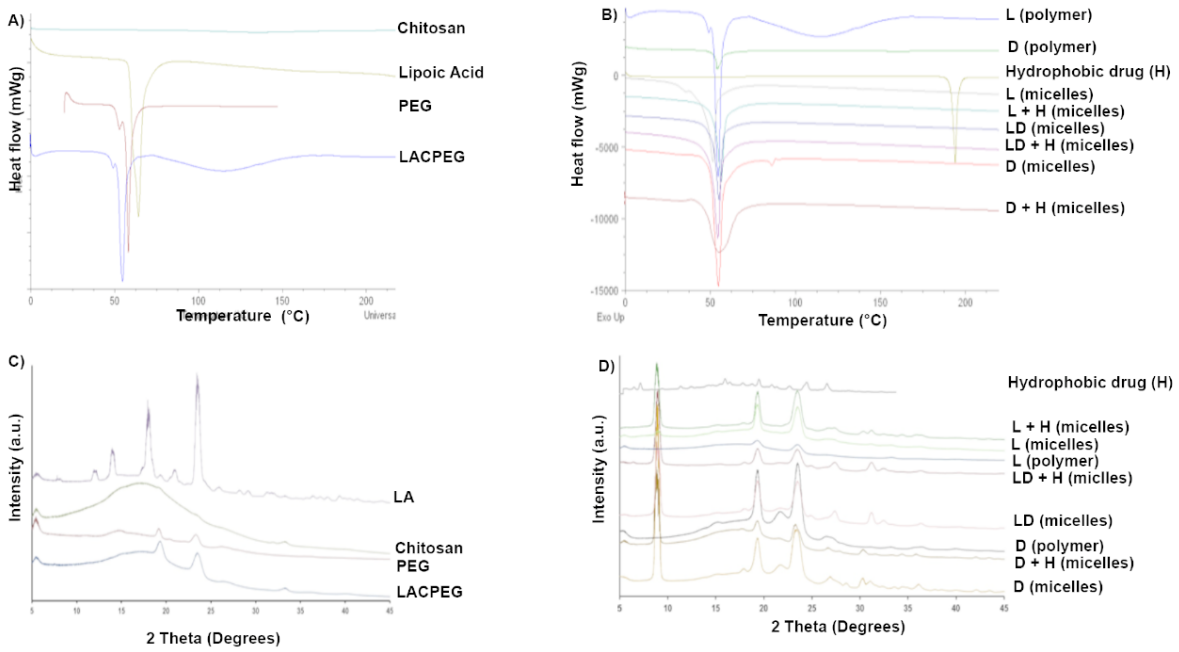

Fig. 4

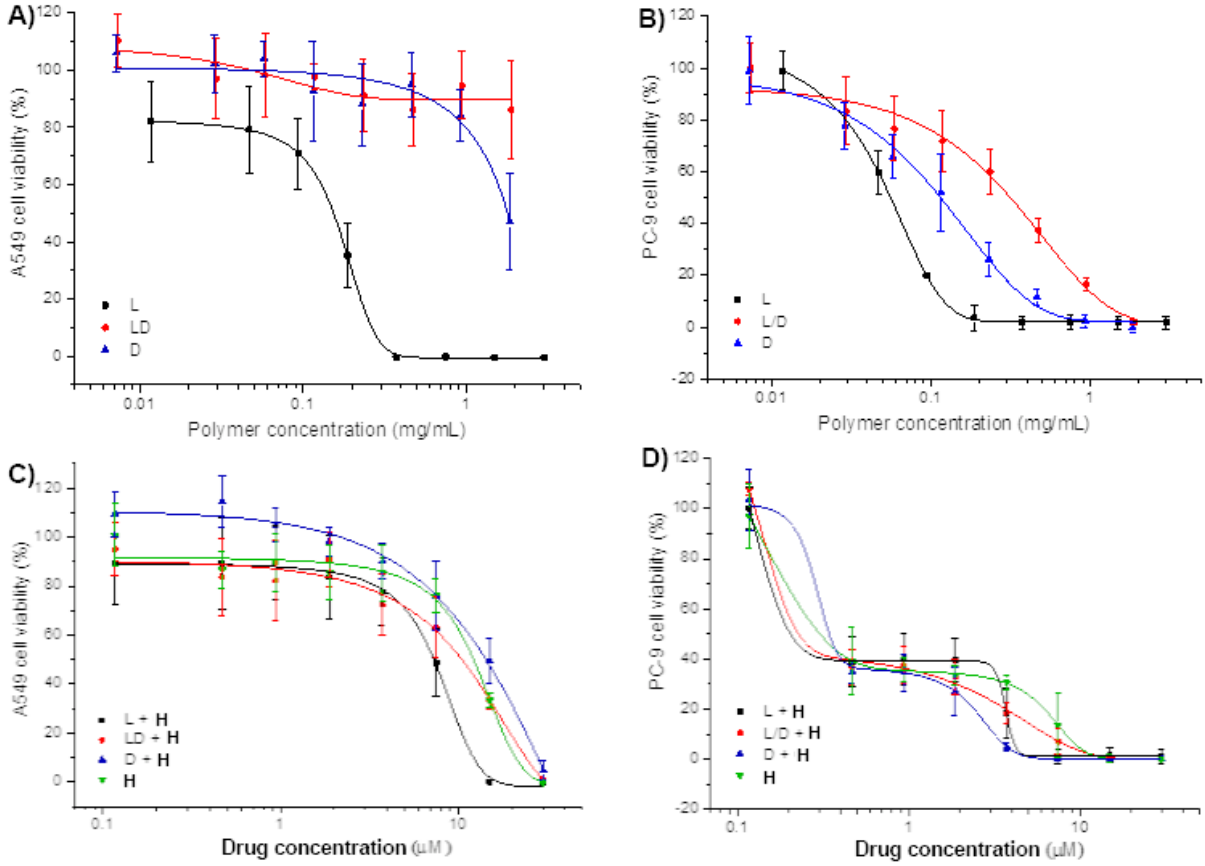

Fig. 5

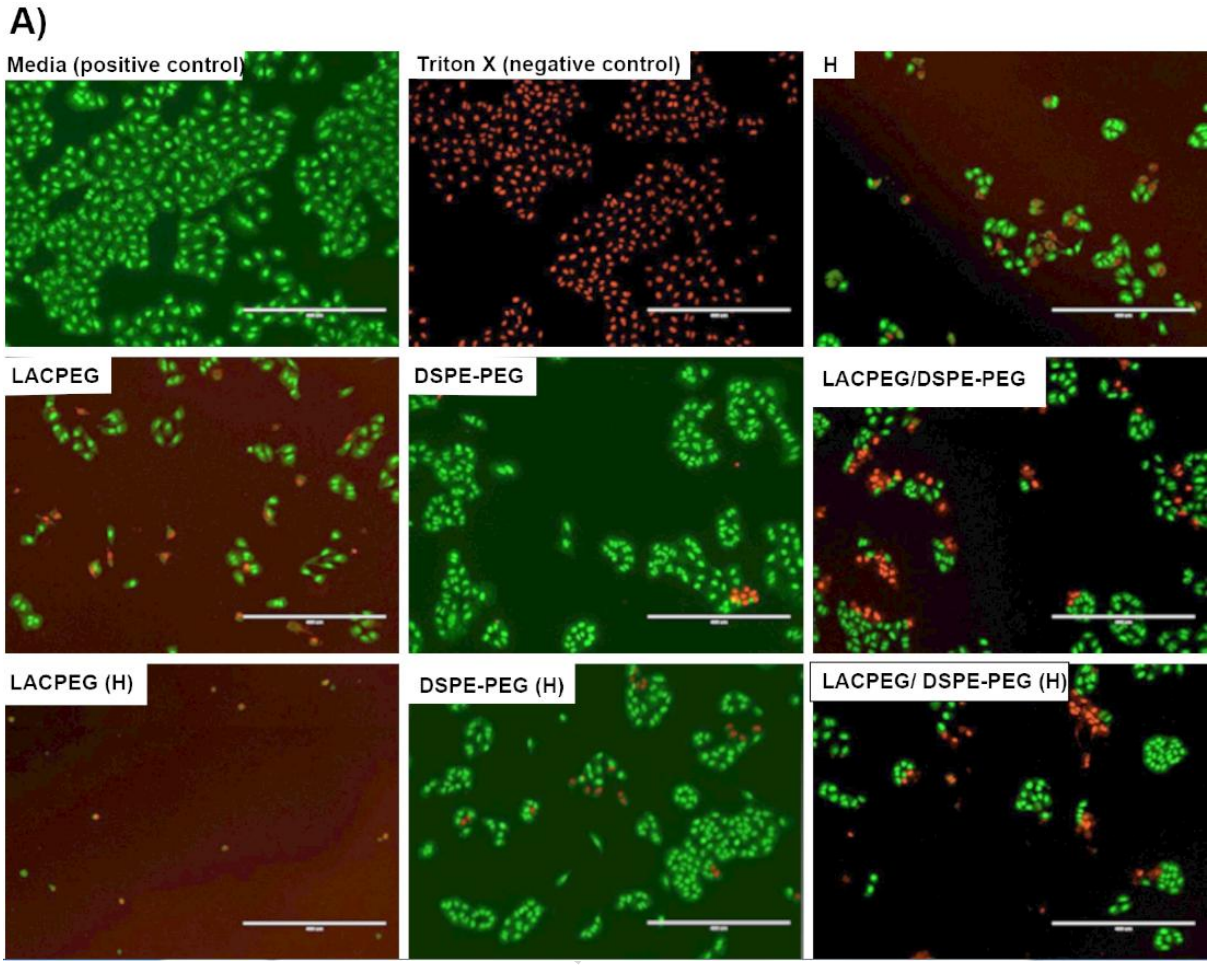

Fig. 6a

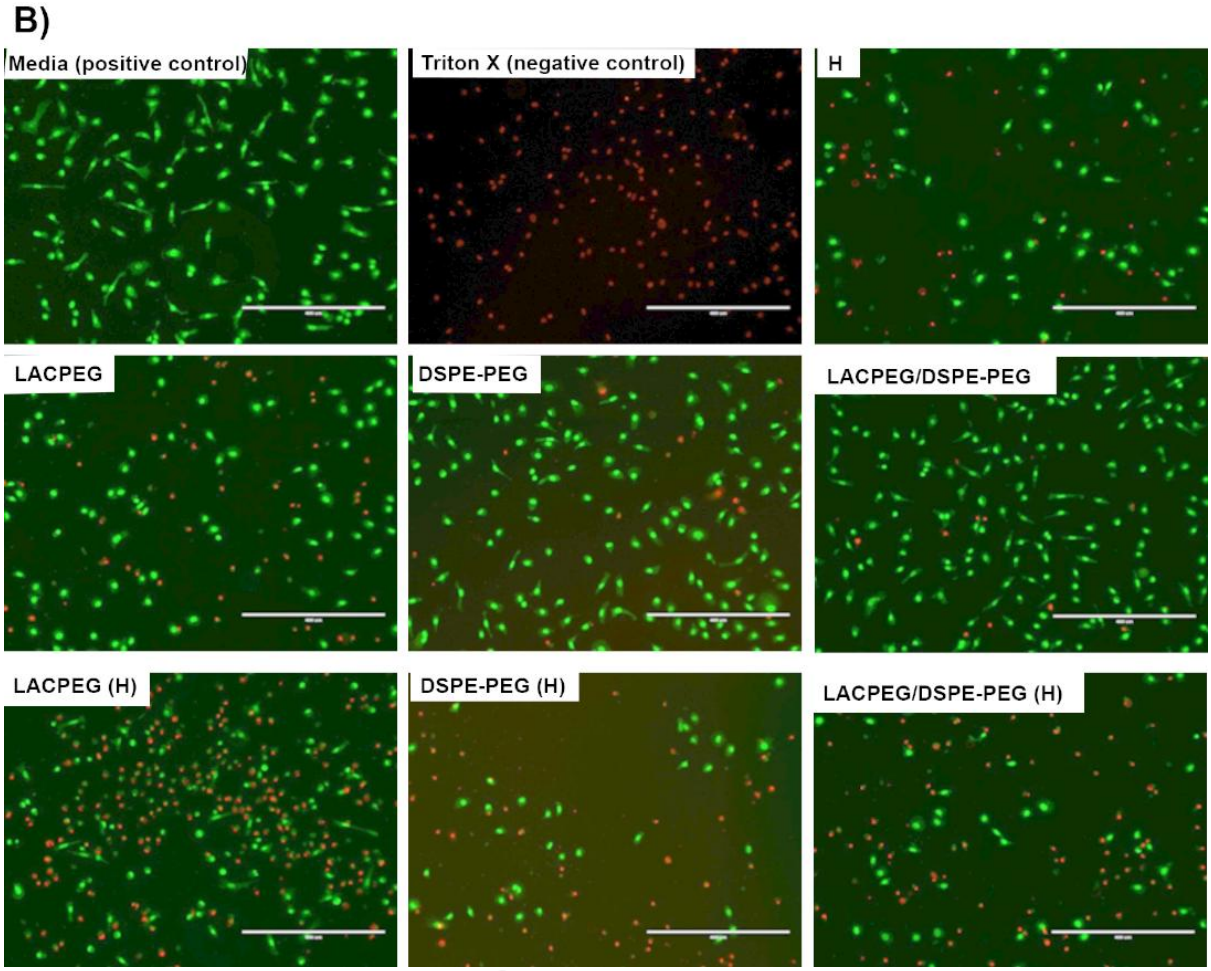

Fig. 6b

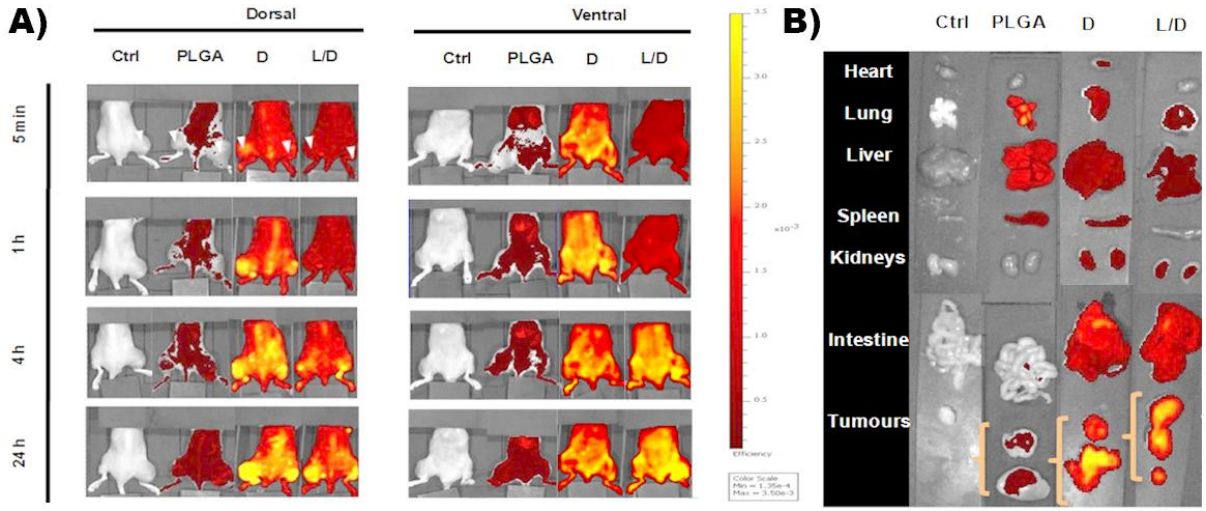

Fig. 7a+b

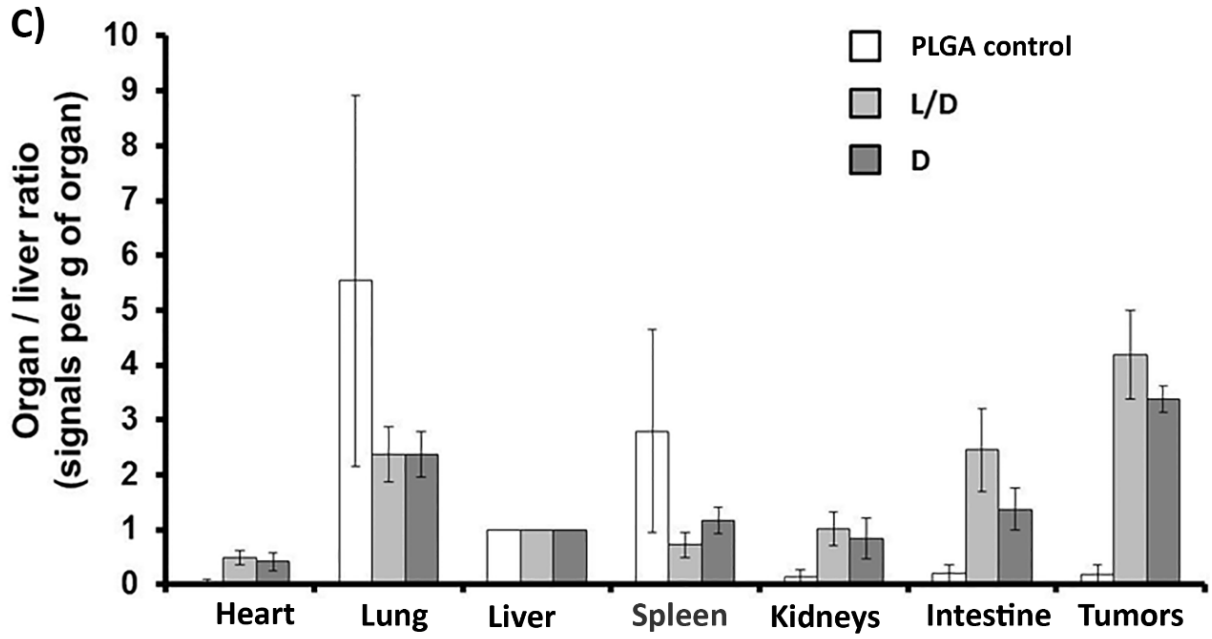

Fig. 7c

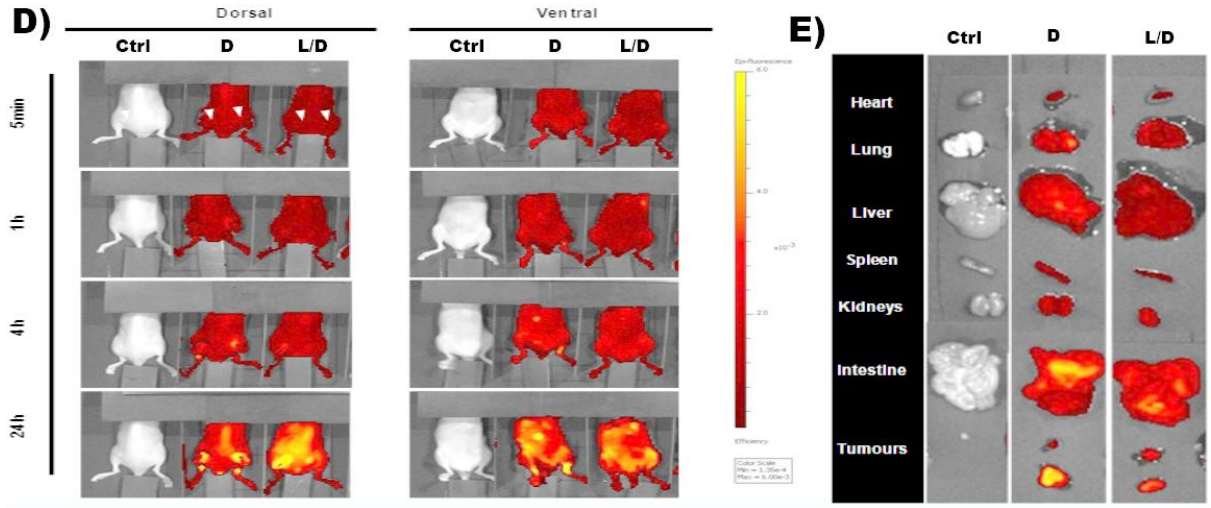

Fig. 7+e

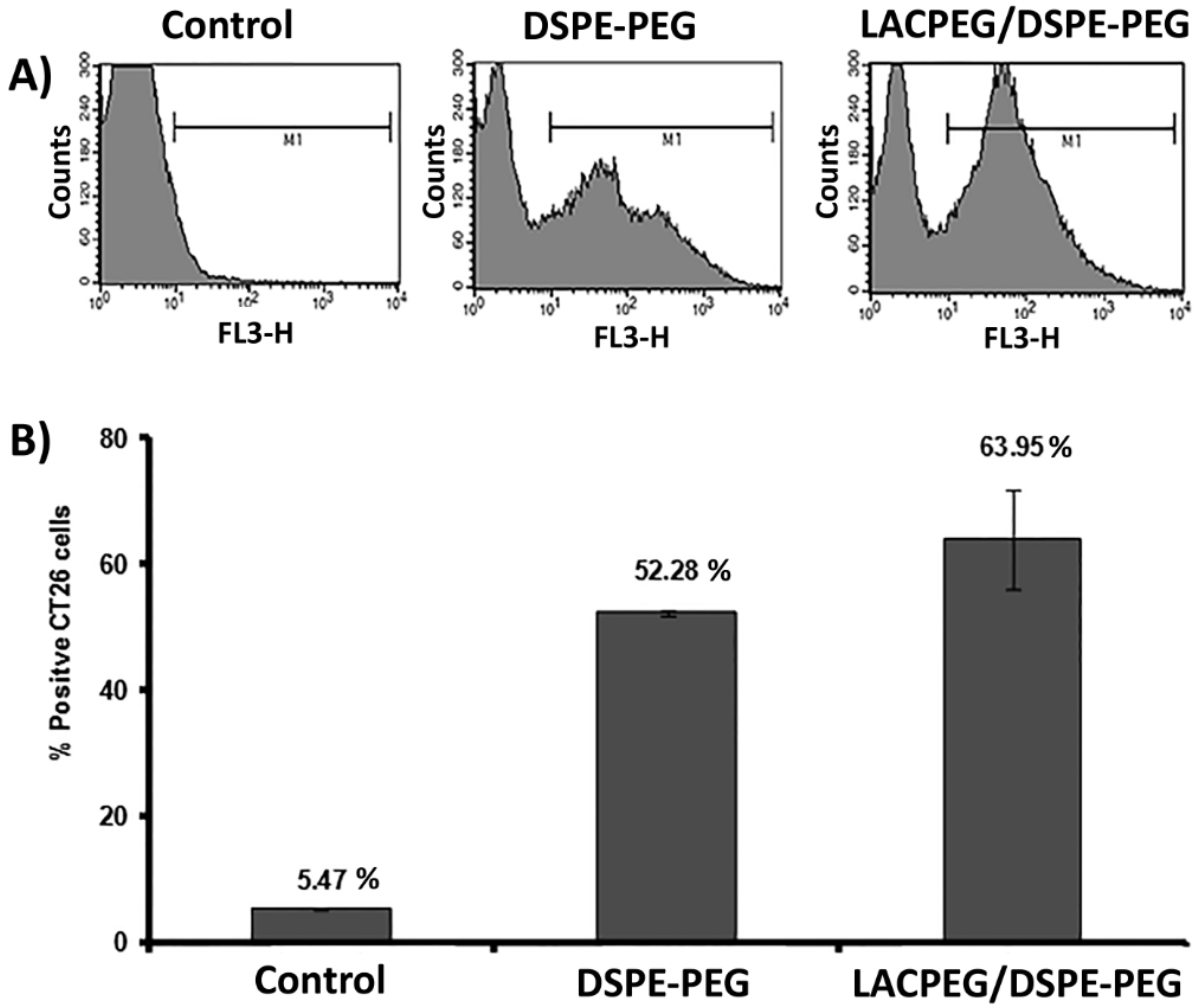

Fig. 8

Graphical abstract